RESOLUTION OF SEISMIC REFLECTIONS

by

ROBERT W. WYLIE
B.S., The Pennsylvania State University
(1954)

SUBMITTED IN PARTIAL FULFILLMENT
OF THE REQUIREMENTS FOR THE
DEGREE OF MASTER OF
SCIENCE

at the

MASSACHUSETTS INSTITUTE OF
TECHNOLOGY

June, 1956

Signature of Author_____
Department of Geology and Geophysics, May 15, 1956

Certified by_____
Thesis Supervisor

Accepted by_____
Chairman, Departmental Committee on
Graduate Students

ABSTRACT

Resolution of Seismic Reflections

by

Robert W. Wylie

Submitted to the Department of Geology and Geophysics on May 15, 1956 in partial fulfillment of the requirements for the degree of Master of Science.

The problem under investigation is that of resolving seismic echoes from two reflecting horizons in the earth where the horizons represent the boundaries of a bed of rock which may be thinning and hence of possible importance as a trap for petroleum. The echoes from the boundaries of a thinning bed are recorded by standard seismic methods as two waveforms which overlap when the bed thins sufficiently. One needs special methods to resolve the two events in these cases.

Assuming that these reflections can be represented as two distinct waveforms or wavelets, the purpose of this thesis was to investigate some approaches to the problem of determining their times of occurrence in the case where overlapping does obscure the second event. A brief discussion of Norman Ricker's papers concerning seismic wavelets and seismic resolution (representing the published work on the problem to date) is presented.

The use of the mathematical inverses of wavelets as contractor operators is investigated and the limitations of such an approach are noted. Such operators should give perfect resolution in a noiseless system. These studies were carried out on theoretical wavelets and on data from a group of reflection seismographs. It was decided that in practice the noise problem is severe.

Another group of experiments is presented representing the uses of a symmetric operator in resolution of our two events. The specific group of symmetric operators which were studied were unfolded cosine transforms of the reciprocals of the amplitude spectrums of the wavelets. In general the results were superior to those obtained from inverse operators but more work is necessary. The limitations and possible applications of the approach are noted along with some suggested future investigations.

Since the above approaches had definite limitations a numerical method for applying a least squares fit was set up and

is presented. Experiments were not carried out on this method and it is left in mathematical form as a future possibility. Computationally the least squares fit method is relatively involved but it is felt that this may be a closer answer to the original problem and that it should be investigated.

Thesis Supervisor:_____

Stephen M. Simpson, Jr.

Title: Assistant Professor of Geophysics

TABLE OF CONTENTS

Table of Contents
(Continued)

Table of Contents
(continued)

page

Acknowledgements

In completion of this thesis it gives me great pleasure to express my gratitude to the many people who's encouragement, suggestions, and efforts helped to make this study possible. Especially I should like to thank Professor S. M. Simpson who's ideas and guidance make up much of the train of thought behind this work. I appreciate also the assistance of Mr. Harold Posen who worked with me on this problem and who's results are incorporated into this thesis. Likewise, I am grateful to Mr. D. R. Grine and Mr. Sven Treitel for the use of their WWI computer programs which made possible the numerical work.

I am grateful to the Geophysical Analysis Group project under which a great deal of this work was done and to which I am indebted for the considerable amount of computer time on WWI which the experiments represent.

The majority of the raw data was supplied by Dr. Dunlap of the Atlantic Refining Company and to him and to Dr. Piety of Phillips Petroleum Company, who's suggestion started this investigation, go my sincere thanks.

Many other suggestions aided the investigation and for these I am indebted to all the members of the GAG project and to the project's sponsors.

Introduction

One of the major problems of interest in exploration seismology is that of establishing the boundaries of a bed which is thinning and may or may not be pinching out. Exploration-wise one or both of these possibilities, pinch-outs or thinning, may be of economic interest in different areas, but in any case the boundaries need to be defined. Much of this mapping has been carried out by intuition and extrapolation from areas in which the boundaries have been established with the maximum resolution of the instruments at hand. Even if a definite answer as to the exact boundaries is unobtainable thereis, nevertheless, much room for refinement of seismic resolution in these areas. By increasing this resolution, extrapolation and intuition need be used to a much lesser extent and uncertainties will be decreased greatly.

The goal of this paper has not been to find a method which will give the exact boundaries but has been to investigate methods of refining the data produced by present seismic instruments in order to obtain greater resolution in pinch-out or thinning areas. Here we are dealing with a specific problem, present over small intervals of seismic records, and have therefore attempted to investigate specific tools which will aid in the solution of this special problem. It is felt that much of the work will be of interest, however, to persons working with more

general questions of seismic resolution.

All of the tools investigated require a much closer inspection of the data coupled with varying degrees of more difficult computation than would be encountered in an ordinary interpretation process. Increasing resolution, however, is quite often worth a great deal of effort. In this investigation the experiments have been carried out numerically on WWI. It is worth mentioning however that, where a numerical method is known to work, large quantities of data are to be studied, and high accurracies are not to be required, electronic analog equipment may often be economically built and put into use.

The investigation is far from complete and I have therefore included descriptions of all the studies so that if the problem is carried on the research can at least start a few steps closer to a final answer. Some of the investigations which proved fruitless are mentioned in a sentence or two where they logically came up in the investigation in order that these blind alleys could be avoided. The experiments concerning methods having possible adaptation in some areas are presented in full.

REVIEW OF PREVIOUS WORK ON CONTRACTION

Our interest in this paper is sighted at improved resolution of two or more signals where their arrival times are such that the first signal is superimposed on the second. We are therefore interested in the character or shape of these signals as they appear on a seismic record so that we might distinguish the arrival of trailing signals which may be obscured by the original reflection wavelet. The signal or wavelet shapes as observed in practice are fairly common knowledge but little work has been published on them. Some work has been done in determining them theoretically.

In 1953 Norman Ricker published two papers in Geophysics(6) (7) concerning the wavelet theory of seismogram structure and wavelet contraction, wavelet expansion, and the control of seismic resolution respectively. In the first of these articles Ricker attempted to describe the action of an imperfect elastic medium on a seismic disturbance using two basic assumptions: first that the initial disturbance at the origin is given by a doublet, and secondly that the disturbance is transmitted according to Stoke's differential wave equation for a visco-elastic medium.

$$\nabla^2\left[\Phi + \frac{4\eta}{3\rho c^2}\frac{\partial \Phi}{\partial t}\right] = \frac{1}{c^2}\frac{\partial^2 \Phi}{\partial t^2}$$

where Φ = elastic displacement

η = viscosity of the medium

ρ = density of the medium

c = wave velocity when η is set = 0

t = time

With these basic assumptions Ricker proceeds to develop theoretical velocity and displacement type seismic wavelets for varying distance relationships. However, many questions have been raised concerning this work. In an interpretation of the paper, Bowman (3) points out four general points of controversy due to some of the mathematics and to the initial and some additional assumptions incorporated in the study. The questions were:

(1). "Are the mathematical parts of the theory on a sound basis?"

(2). "Does experiment bear out the theory?"

(3). "How does the non-realization of the assumed original pulse shape in practice affect the applicability of the theory?"

(4). "What is the physical meaning of the assumed wave equation?"

In general the answers to the above questions as partially offered by Bowman and others seem to support the mathematics but indicate a reasonable amount of doubt as to the actual occurrence of Ricker type wavelets in field studies. Strong objection has been made due to the

difference in Ricker's model of the earth from the actual and to the lack of field evidence supporting his theoretical damping conclusions.

Ricker's experiments and theory were based on an earth model which was visco-elastic. As far as this earth model is concerned Ricker's theory has been shown to be correct. Ricker's experiments were carried out on the Pierre Shale and in this area there was a very good agreement of theory and observed data. However the properties of Pierre Shale differ from most rocks in that this shale is almost truly visco-elastic. Jeffreys (4) pointed out the non-visco elastic state of most rocks and the fact that a more complicated wave equation was in order. Van Melle (10) and Treitel (9) have shown that the wave equation used by Ricker is also non-physical from the energy relationships.

In his second paper in 1953 Ricker incorporated the study of his wavelets into a paper concerning seismic resolution. Using these wavelets as models Ricker considers a seismogram, free of distortions, as being made up of large numbers of fundamental wavelets with different time origins superimposed on one another. The analysis of a seismogram he then considers as the breaking down of the record into its wavelet components. To do this, Ricker proposes a wavelet contractor as an electronic filter, which when coupled with proper recording techniques would produce a distortionless seismogram. The individual wavelets on such a seismogram would be contracted to a

lesser breadth without altering the relative arrival times of the wavelet centers. Ricker set down two conditions which were to be met within the band of relavent frequencies.

First: The phase characteristic must be a linear function of the frequency f with intercept on the phase axis of zero or an intergral multiple of π. For the wavelet to emerge erect, the phase intercept should be zero or an even multiple of 2π.

Second: The amplitude response characteristic must be of the form $A = A_o e^{kf^2}$ where f is the frequency and A_o and k are constants.

In-as-much as the characteristics of this wavelet contractor have been derived from the wavelet theory which has been seriously questioned a great deal of reserve must be used in evaluating the usefulness of the method and the equipment. It was shown by Robinson(8) that Ricker's wavelet contractor could be duplicated by a mathematical linear operator. Using Ricker's conditions and assumptions Robinson achieved the same results. On actual seismograms the maximum contraction achieved by Ricker's contractor was approximately 0.8 of the original breadth. Within this range Ricker's contractor, even with its non-physical basis, seems to have applicability and sufficiency for seismic studies. It was hoped, however, that we might find a better method of seismic resolution using a different approach which did not incorporate some of the weakness

of Ricker's assumptions. This thesis study was launched to accomplish this.

II Formation of an Inverse

In transforming the seismic recordings through his contractor Ricker 's operations required that the shape of the wave forms remain constant. It was felt that if this condition were dropped better contraction and / or resolution could be affected with no loss of information pertaining to the onset times of the reflected energies. This was the general problem and the study proceeded historically in almost the same pattern as this thesis.

The operation which we are searching for is one which will give a better indication of the time of onset of seismic reflections. As in most studies we have assumed that the seismic traces as time functions may be represented as a noise function plus signal functions whose time origins are directly related to the geometries and the velocities involved. Finding these onset times is the broad problem. Discovering them in areas where they are not visible on the seismic record due to interference from other signals and noise without destroying the information from other signals is the specific problem. The most practical uses of such a method is of course that of finding the onsets of two overlapping reflections such as would represent a pinch-out or thinning of a bed bounded by two reflecting horizons. It was with these goals in mind that we proceeded. Considering the reflection from any horizon to be a finite time series and having relaxed the condition for constancy of wavelet shape, it was then quite logical to attempt to find an operator which would produce a spike or near spike at the onset of the waveform and which would produce negligible output before and after this onset. These characteristics suggest the mathematical inverse. This inverse when convolved as a series term by term with the original series will produce a series which will be an impulse

followed by zero terms. In finding an inverse for a time series one merely performs a polynomial division into unity obtaining a polynomial whose coefficients are the desired inverse.

$$a_o + a_1 z + a_2 z^2 + a_3 z^3 \ldots \; \overline{/1}$$

where a_o, a_1, $a_2 \ldots a_n$ are the ordinates of the wavelet.

Unfortunately, as was found by experiment, most inverses of waveforms found on seismic records are unstable. That is to say, the higher order terms in the true inverse polynomial become increasingly divergent. These divergent series will of course theoretically still give a perfect spike when convolved with the original wave form if one retains the infinite series of the inverse whose terms diverge also to infinity. Again there is a logical compromise. As suggested by Dr. Piety (5) we need only use the first group of smaller terms in our inverse to produce a spike in convolution which will be valid to the number of terms used from the inverse. This restriction may or may not be serious in application depending upon the instability of the inverse and the interval length over which we wish to operate.

Experiments were then set up to test the applicability of our proposed "chopped-off" inverse. Two waveforms were chosen for the initial study from Ricker's theoretical wavelet tables. They were the Ricker wavelet "taken at infinity" and the Ricker wavelet "taken at twenty-five" which we shall henceforth respectively denote as V(∞) and V(25). These wavelets were modified so that there initial values represented a discrete jump in amplitude, the original waveforms as derived by Ricker having extended in time from minus to plus infinity. This modification was necessary in order that any stability

might be achieved by our inverse and it does render the wavelets more physical. -- In our notation we will designate $1/V(\ )$ as the inverse.-- Using these modifications (Fig. 1) the two wavelets were divided into unity and 180 terms of $1/V(25)$ and of $1/V(\infty)$ were calculated in order that we might observe the nature of the instability. (Fig. 2 and 3).

The stability of the inverse of any symmetric wavelet and hence the true stability of any symmetric wavelet has been shown to be impossible (MIT GAG Report 9, Section 4 (1)) and hence the instability of $V(\infty)$ was known. In general, if any of the roots of the z plane transfer characteristic lie within the unit circle the wavelet has an unstable inverse. This was shown to be the case for $V(25)$ also by observing the nature of the computed inverse (Fig. 2 and 3). We note that in Fig. 3 the inverses appear to be time series added on to exponential functions. As we are only interested in the first portion of our inverse this exponential function has been determined and subtracted from the raw inverse in various ways in attempts to create an inverse which would be valid over a wider range of convolution.

The logarithmic plot of the inverses (Fig. 3) shows the exponential dependence very clearly. The functions ae^{bx} and $a(e^{bx}-1)$ were determined by fitting the asymptotes of $1/V(25)$ and $1/V(\infty)$ to straight lines on this logarithmic scale. In subtracting these exponential functions, the term -1 has little effect on the large terms of the inverses but it does tend to render the first values , which are the most important in this study, more similar to the exact inverse. In. Fig. 4 we show the effect of retaining consistency in the first terms. Here we have reinverted the modified inverse of $V(25)$ and $V(\infty)$ and have found

$$\frac{1}{\frac{1}{V(25)} - a(e^{bx}-1)} \qquad \text{and} \qquad \frac{1}{\frac{1}{V(\infty)} - a(e^{bx}-1)}$$

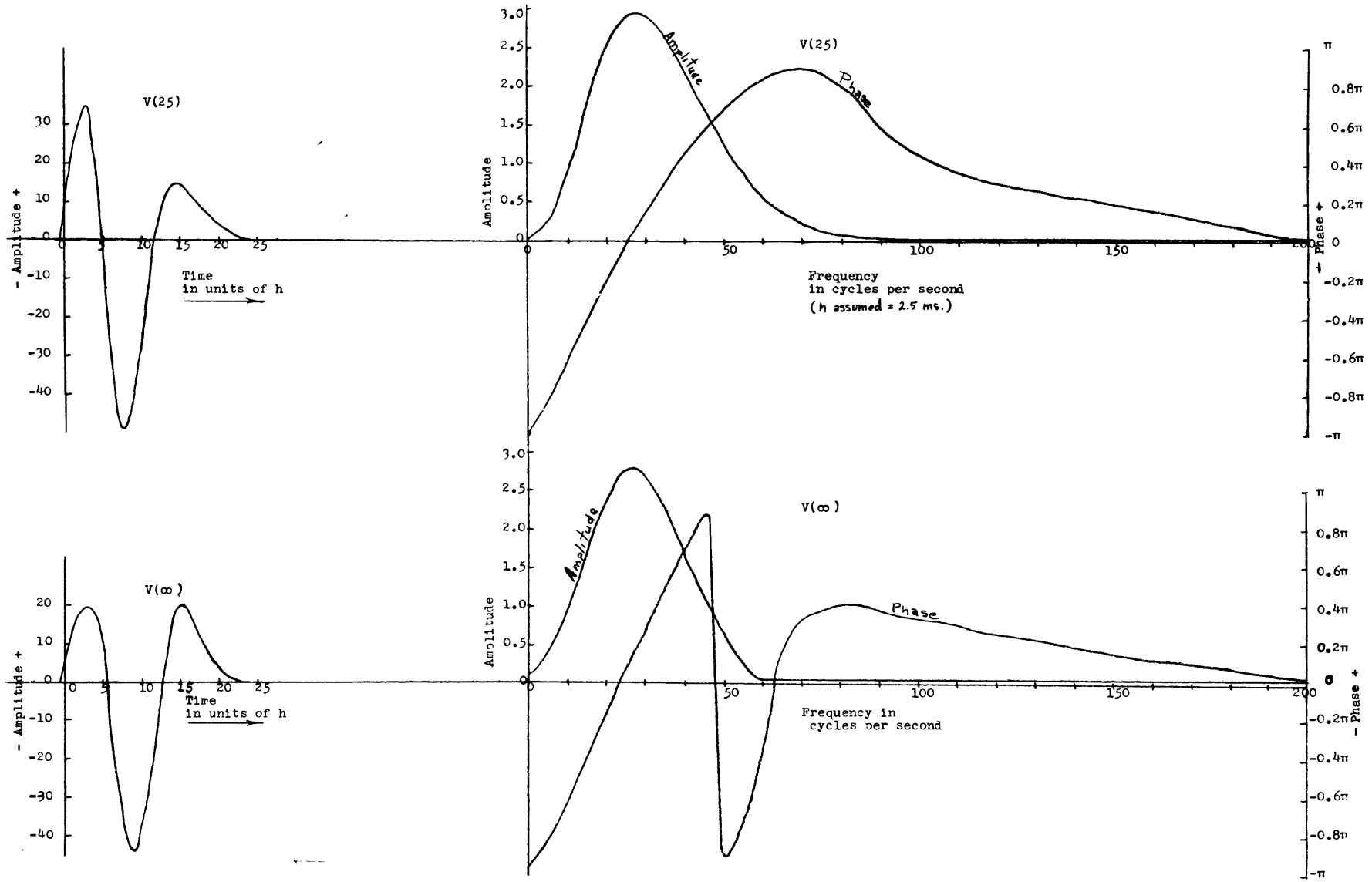

Fig. 1 Ricker Wavelets V(25) and V(∞) with their spectral characteristics.

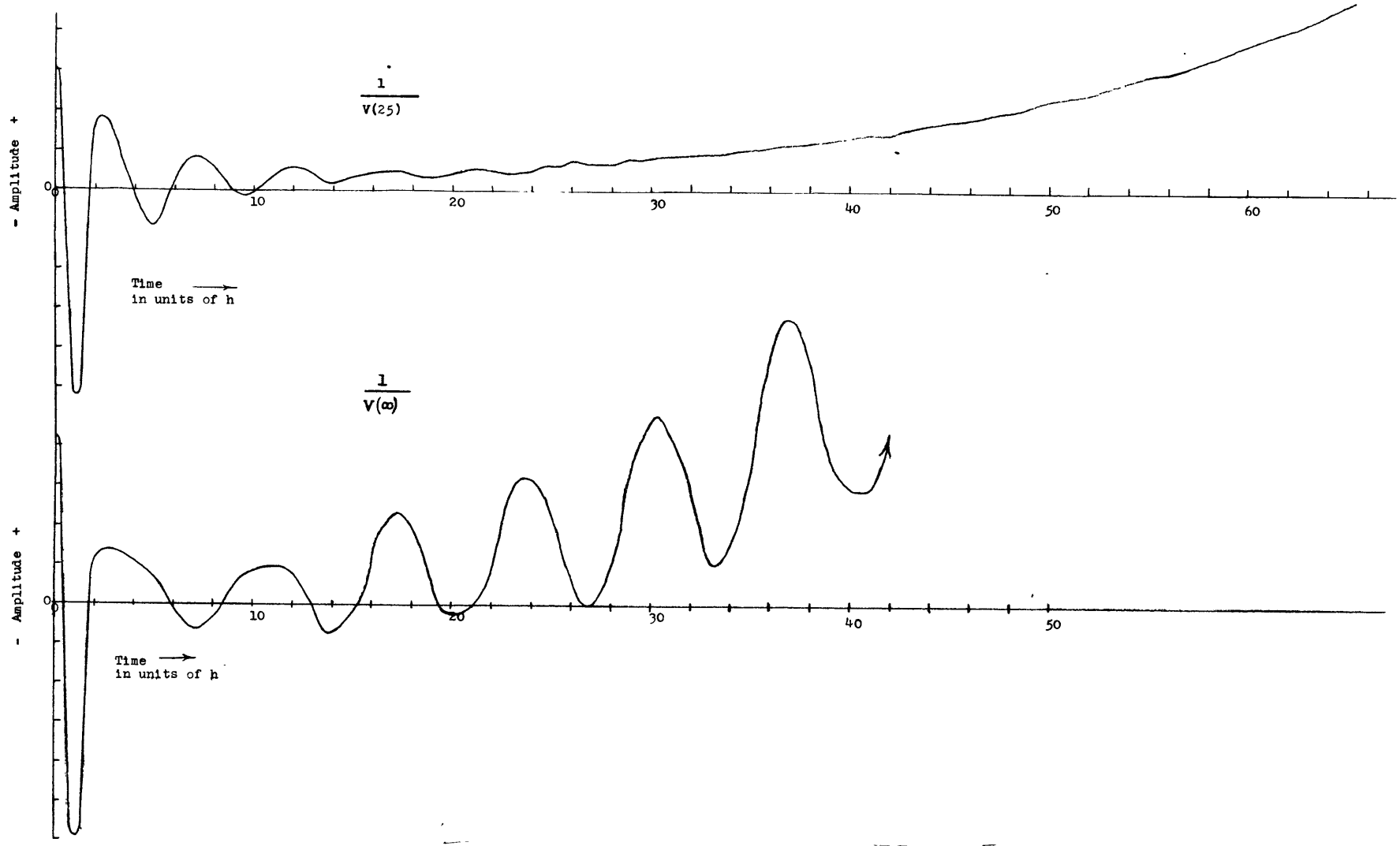

Fig. 2 Computed inverses to V(25) and V(∞) of **Fig. 1**

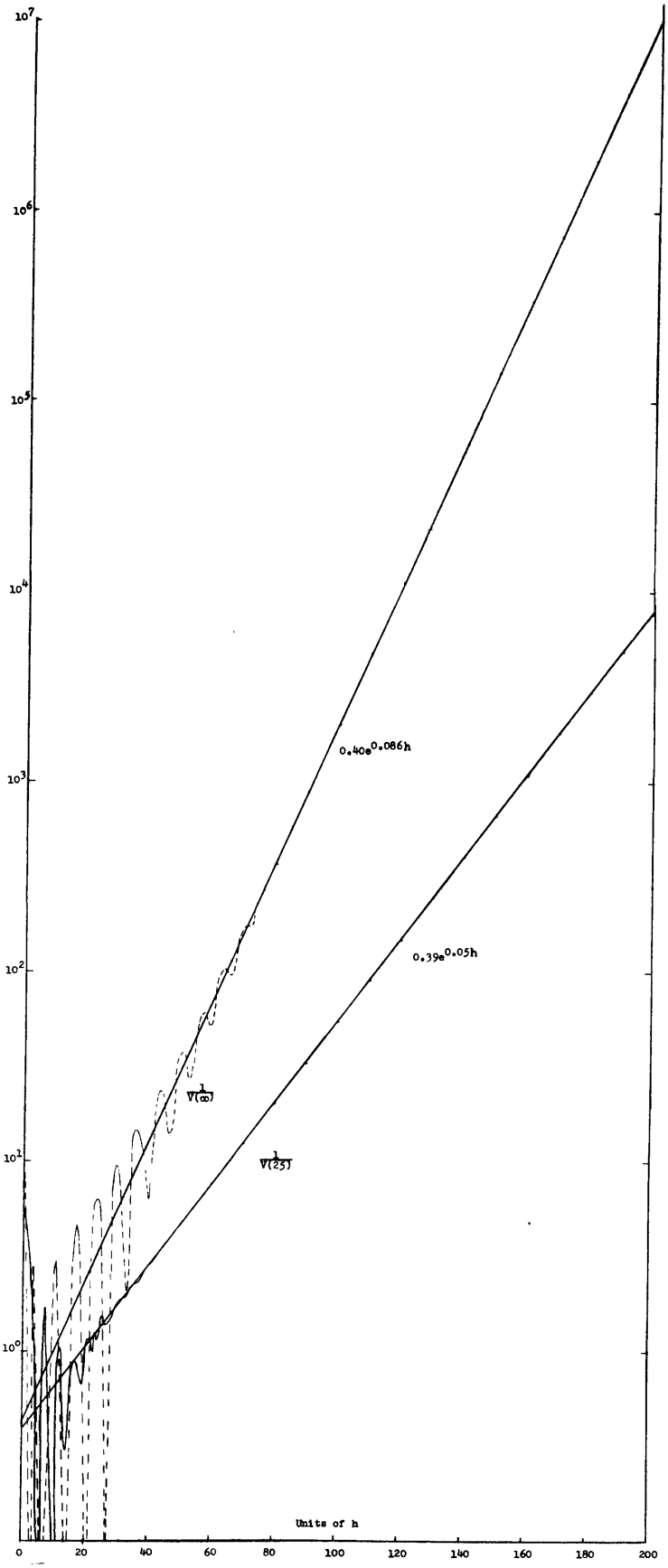

Fig. 3 Inverses of V(25) and V(∞) showing exponential divergence

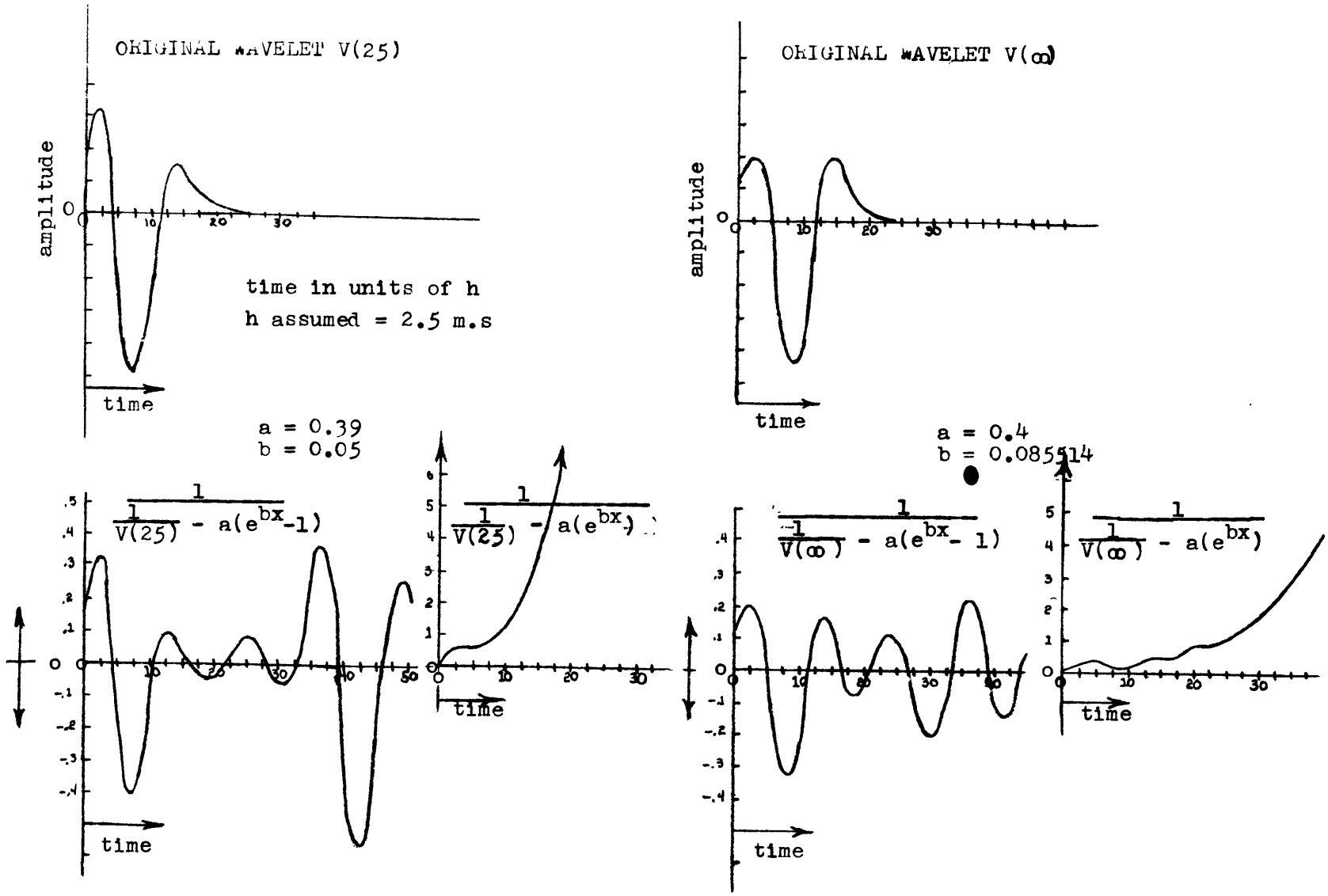

Fig. 4 Comparisons of re-inverted approximate inverses with original wavelets

to be substantially similar to V(25) and V(∞) whereas

$$\frac{1}{\frac{1}{V(25)} - a e^{b\alpha}} \qquad \text{and} \qquad \frac{1}{\frac{1}{V(\infty)} - a e^{b\alpha}}$$

differ from the original wavelets completely.

The question also came up as to whether the inverse was not just an exponential plus the inverse of the stable wavelet whose amplitude spectrum was the same as that of the original wavelet (Fig. 1). Using a factorization program developed by other members of the GAG project this wavelet and its inverse were formed (Fig. 5) from report 10b MIT GAG project. As we can see in Fig. 6 this guess proved to be false.

As a result of these experiments the modified inverses

$$\frac{1}{V(25)} - a\left(e^{b\alpha} - 1\right) \qquad \text{and} \qquad \frac{1}{V(\infty)} - a\left(e^{b\alpha} - 1\right)$$

were used in further studies. These are shown with their amplitude and frequency spectrums in Fig. 7. It can be noticed in Fig. 3 that V(25) seemed more stable than V(∞). This was interpreted to indicate the probability that the anomalous roots of the characteristic polynomial of V(∞) were further inside the unit circle than those of V(25). The amplitude and phase characteristics of the modified inverse of V(25) at high frequencies are close to what we would expect for a true inverse (amplitudes related reciprocally, phases being the negative of each other) but the phase condition breaks down at low frequencies. The spectral characteristics for V(∞) and its modified inverse do not fit these conditions as well. This phenomena would seem to indicate that convolving the modified inverses with the original wavelet will produce a spike plus low frequency. The results of this convolution are shown in Fig. 8 and the preceding analysis is shown to have been correct.

Using these convolved results we then proceeded to set up a theoretical noiseless seismic situation with V(25) in

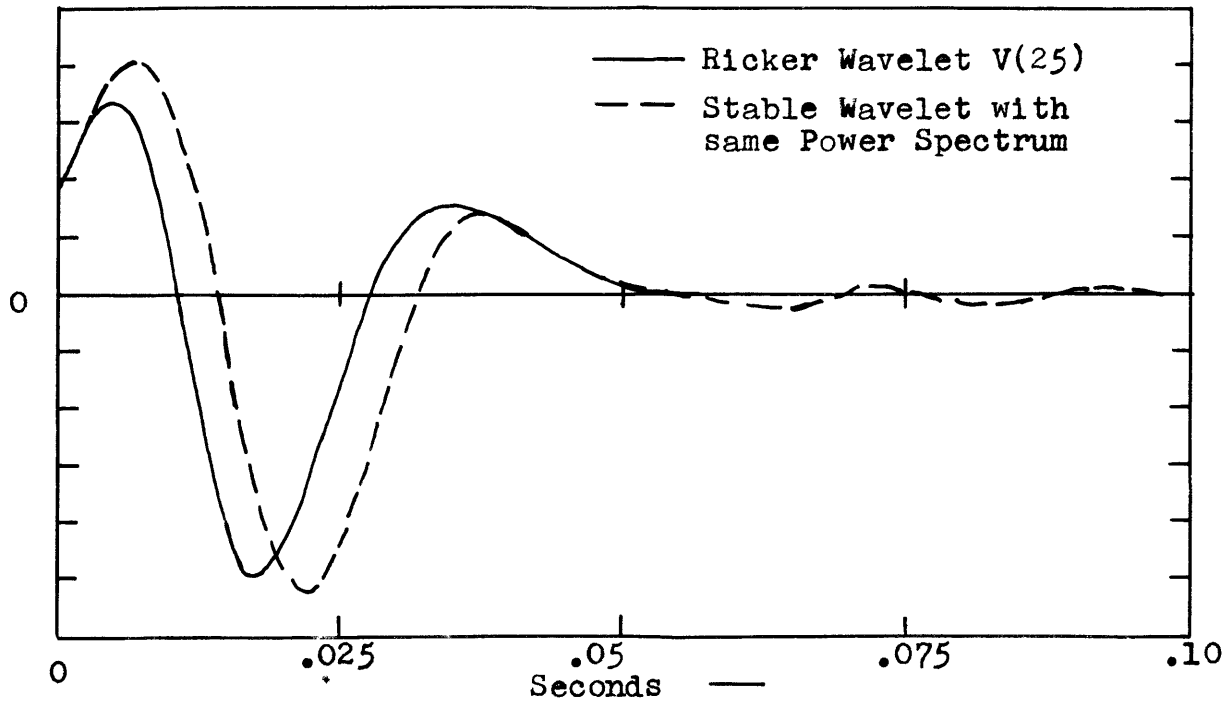

STABLE AND UNSTABLE WAVELETS Fig.

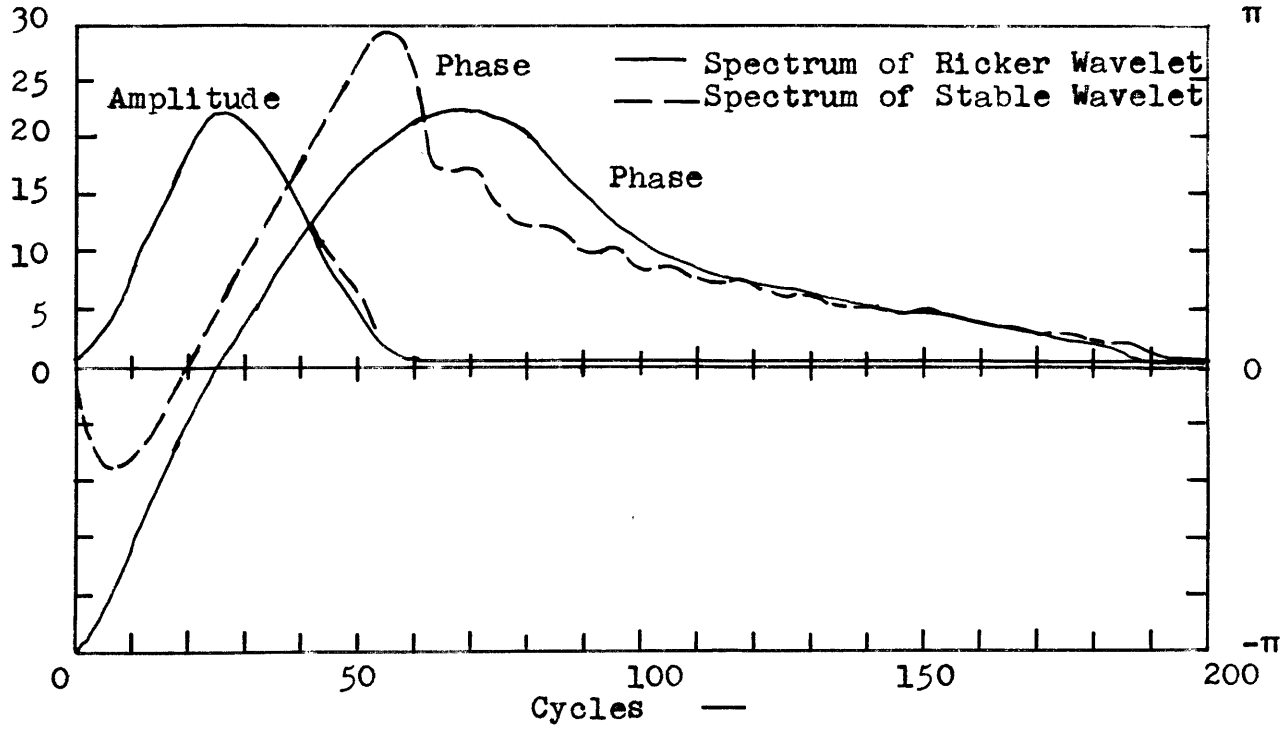

CORRESPONDING AMPLITUDE AND PHASE SPECTRA Fig.5

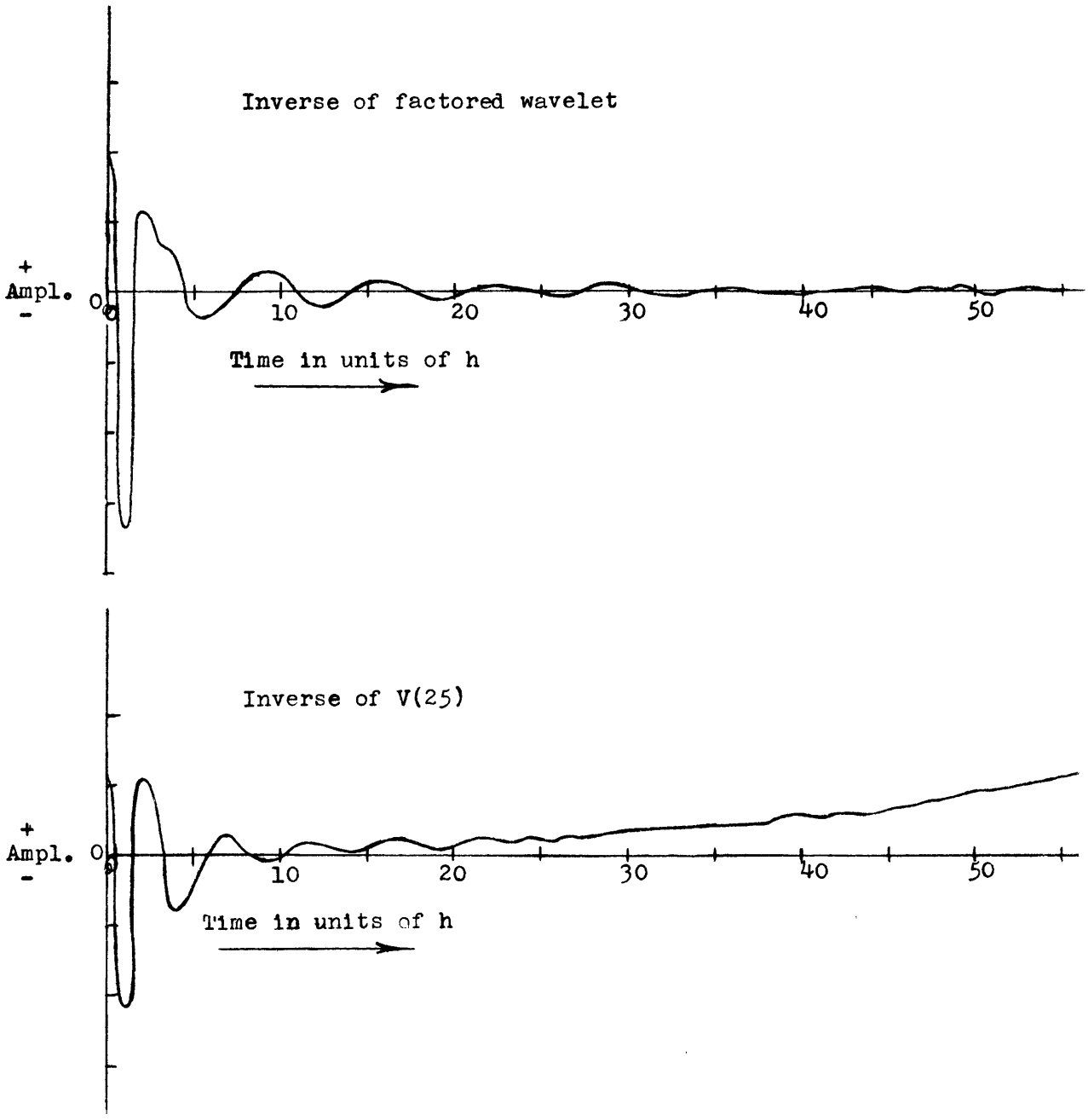

Fig. 6 COMPARISON OF $\frac{1}{V(25)}$ WITH THE INVERSE OF THE STABLE WAVELET ASSOCIATED WITH THE AMPLITUDE CHARACTERISTIC OF V(25)

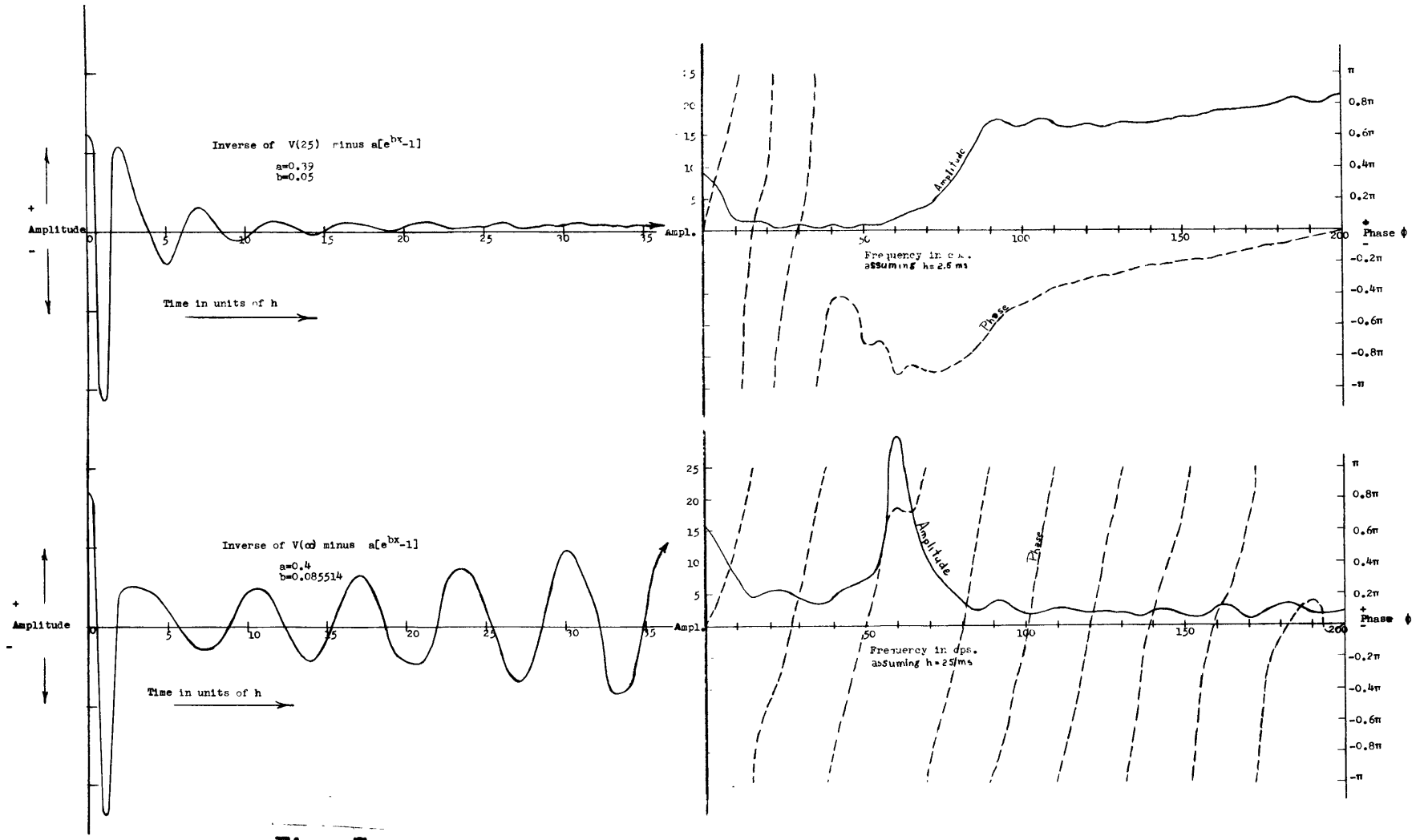

Fig. 7 Smoothed inverse operators and their spectral characteristics.

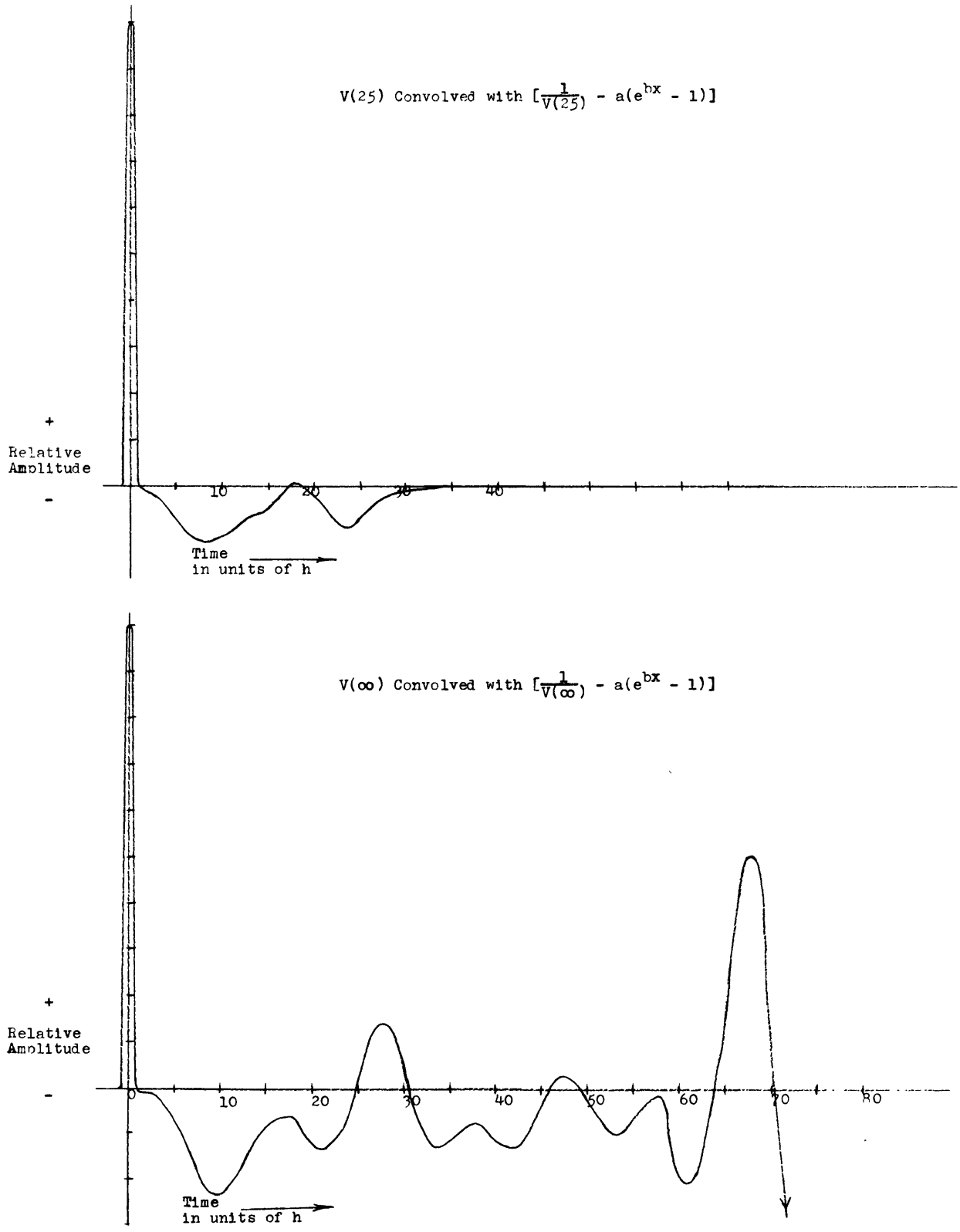

Fig. 8 **Convolutions of V(25) and V(∞) with their approximate inverses**

order to show its possible use under ideal conditions. These results are shown in Fig. 9. In this test we assumed that a Ricker wavelet occurred on a noiseless section of a seismic trace and that after a time lag another positive or negative V(25) of different amplitude occurred. The resulting combination hid the second event in both cases. Using the modified inverse as an operator a convolution was made and definite resolution was produced.

This was of course an ideal case where the first and second wavelets were similar, in phase, and where there was no noise. As our data is taken at discrete intervals in digitalizing any seismic information we were first interested in the effects of phasing. The occurrence of any reflection over a seismic record will have different onset times on various traces. We must of necessity continue our digitalization at a constant spacing over the interval of interest on the seismic record or traces. It is obvious, therefore, that we very seldom hit the first term of our wavelet with a data point. It is this first term which our inverse has been developed to spike and hence there is need to study the sensitivity of the approach to a shifting. Such an experiment was carried out on V(25) for shifts of 1/4, 1/2, 3/4 and 1¼ and the results are shown in Fig. 10. There appears to have been a shift in the convoluted results and some slight changes in amplitudes. The characteristics are still quite good however. The data points of V(25) appear to be close enough together and 1/V(25) insensitive enough to small changes that we can conclude that for this operator and wavelet phasing is of only minor importance. In a later section of this paper we shall see how the spread of the data points can make the phasing a major problem.

The problem of noise or variation in wavelet shape

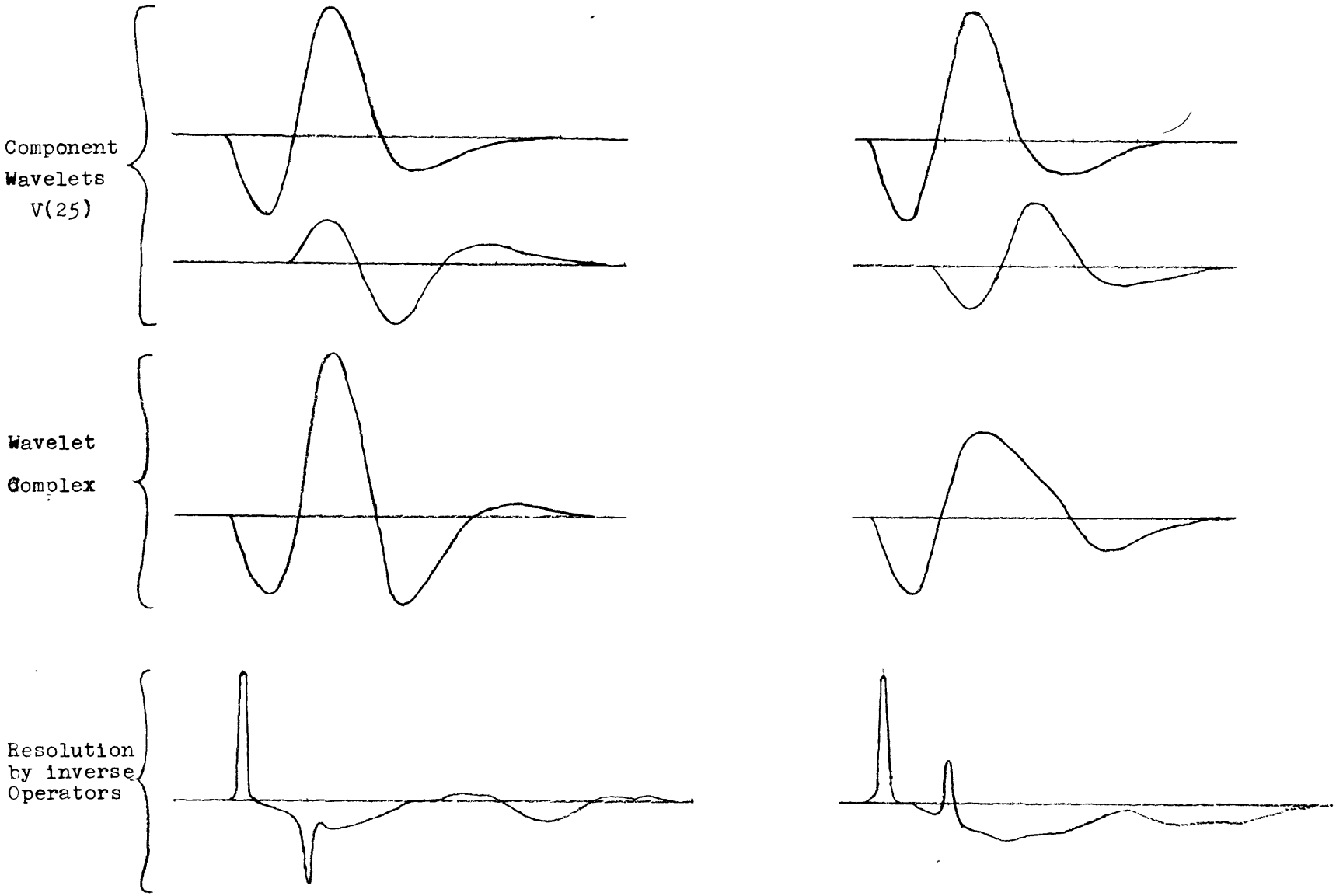

Fig. 9 **Artificial wavelet complexes and their resolution by inverse operators**

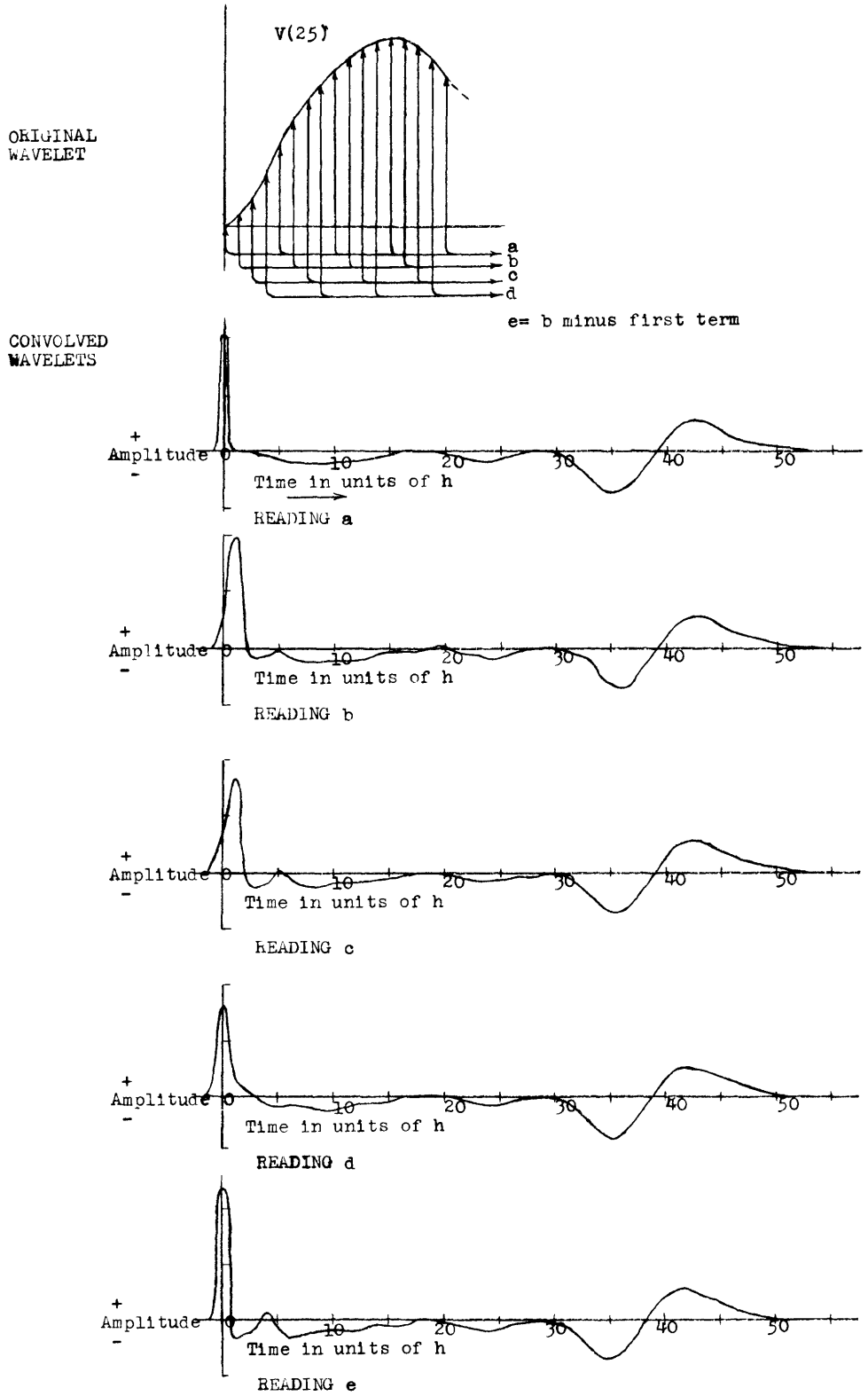

Fig. 10 Phasing test. Inverse operator of wavelet from readings (a) convolved with wavelets from readings in different phase relations

appears to be much more critical in the case of our inverse operators. If there were only the original wavelet for which we had established an inverse followed by another waveform in our interval of interest we would still be in good straits. The first waveform would produce a spike followed by a relatively flat period until the onset of the second waveform which in convolution would at worst produce a transient. This ideal case is in practice unobtainable as we invariably have some noise which will distort the shape of the first waveform. This will vary also from trace to trace. In order to discover the effects of this phenomenon a convolution was made with the modified inverse of V(25) and V(∞) and the modified inverse of V(∞) and V(25). These results are shown in Fig. 11. The modified inverse of V(25) appears to be relatively insensitive to changes in shape compared to the modified inverse of V(∞). Even the former points out definite limitations of this process in situations where we must contend with noise.

The operation must be sensitive enought to indicate the onset of a set waveform but not sensitive to the degree that it will blow up when it is convolved with a wavelet other than its inverse. Thus if we were concerned with wavelets of the same form as V(25) we would appear to have solved our general problem. Ricker points out, however, that ordinary seismic filters do not yield wavelets of the same form as V(25). They are more likely of the form shown in Fig. 13. It should be pointed out also that this dissimilarity of waveforms may not be totally electronic and as stated previously the occurrence of Ricker's wavelets in actual practice is questionable. Going back to Fig. 1 and noticing the form of V(25) there is reason to expect difficulties in applying the inverse operator approach to contracting waveforms usually observed on seismic records. Most waveforms in practice do not have their maximum

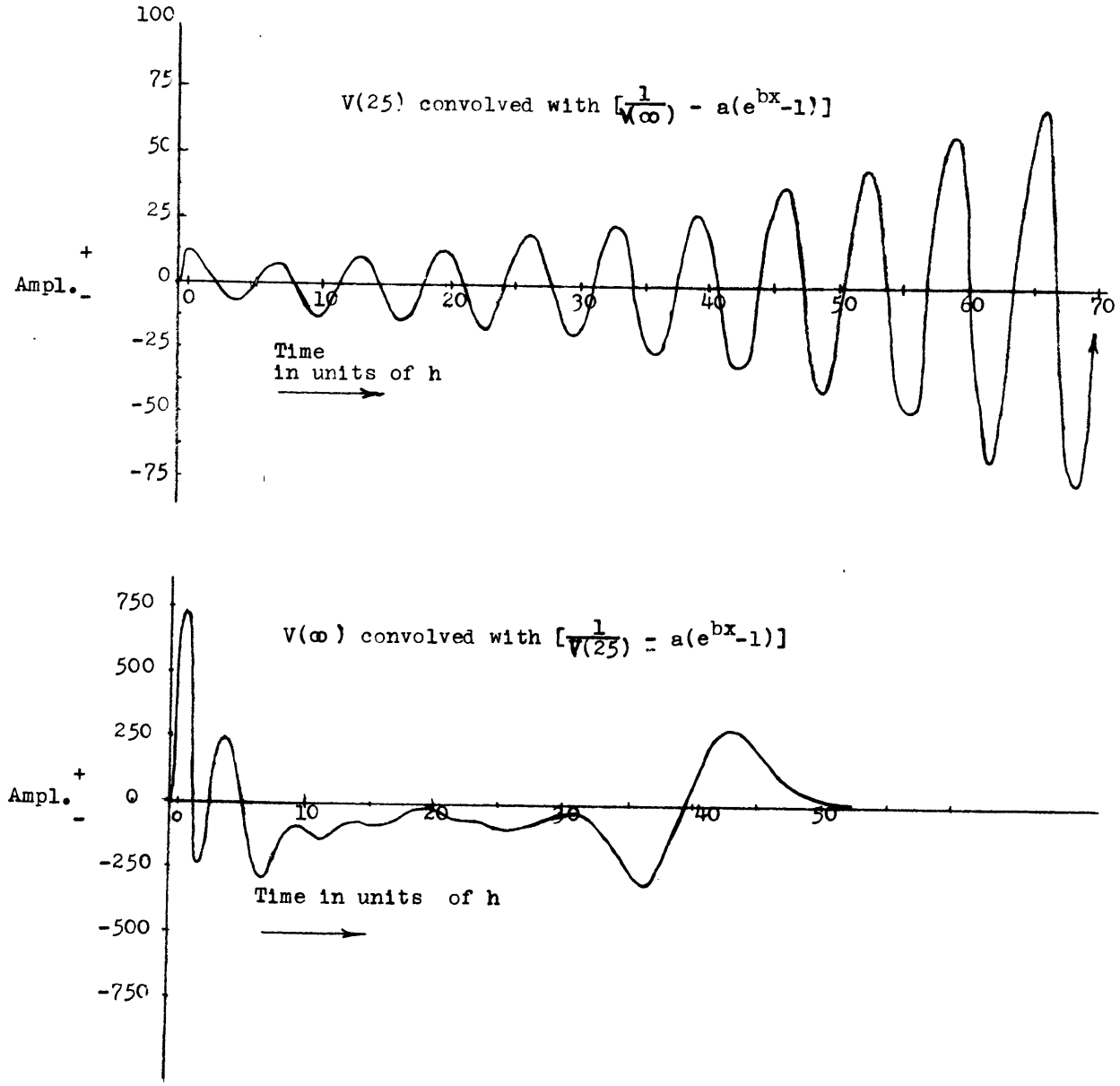

Fig. 11 **Results of convolving approximate inverses of V(25) and V(∞) with V(∞) and V(25) respectively.**

amplitudes within the first few terms. Usually they build up to maximum values in later terms, a characteristic which will tend to increase the instability. One would expect the inverses of these waveforms to diverge quite rapidly.

In order to study the overlapping of two waveforms from an actual seismogram a suite of records was obtained from the Atlantic Refining Company which exhibited several pinch-out structures. Of these we chose four records for our study (Fig. 12). The reflection picks at 0.98 and 1.07 seconds on record 7.19 were seen to get closer and closer together as we moved over horizontally to record 7.16 where they seemingly combined into one wavelet complex at 0.98 seconds. Analysis was started on the two distinct waveforms which were present on record 7.19.

The first waveform appearing around 0.98 seconds on record 7.19 was averaged over this record by lining up the maximum positive peaks on every other trace, digitalizing each over a fairly wide range, and averaging these time series term by term (Fig. 13). Thus we have assumed that the noise is uncorrelated on the average with the signal. The averaged wavelet was then modified so that it would have a definite zero origin and would tail-off to zero. It is noticed on Fig. 13 that the averaged wavelet from 7.19 has its largest positive amplitude not in the first swing as did V(25) but rather in the second positive form later in time. This is much more in line with the results of other field observations.

An inverse was calculated for this modified wavelet (Fig. 14) and as predicted it was widely divergent after only the first few terms. The nature of the terms in this inverse also show no signs of possessing any generalized smoothing function such as $a(e^{bx}-1)$ which was so useful in rendering the inverses of the Ricker wavelets stable over long intervals of time.

7.19 7.18 7.17 7.16

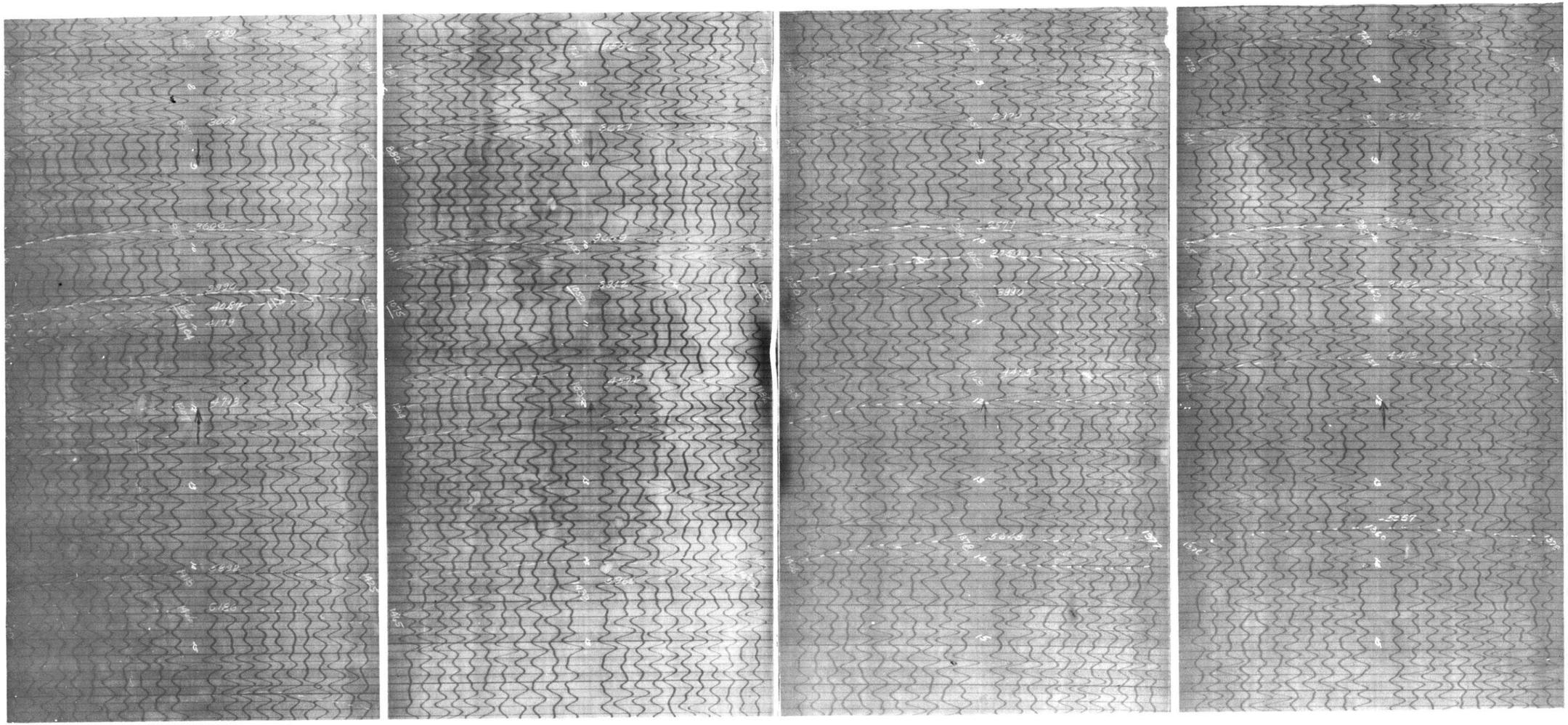

Fig. 12 Four records of the Atlantic Refining Co. exhibiting pinchout.

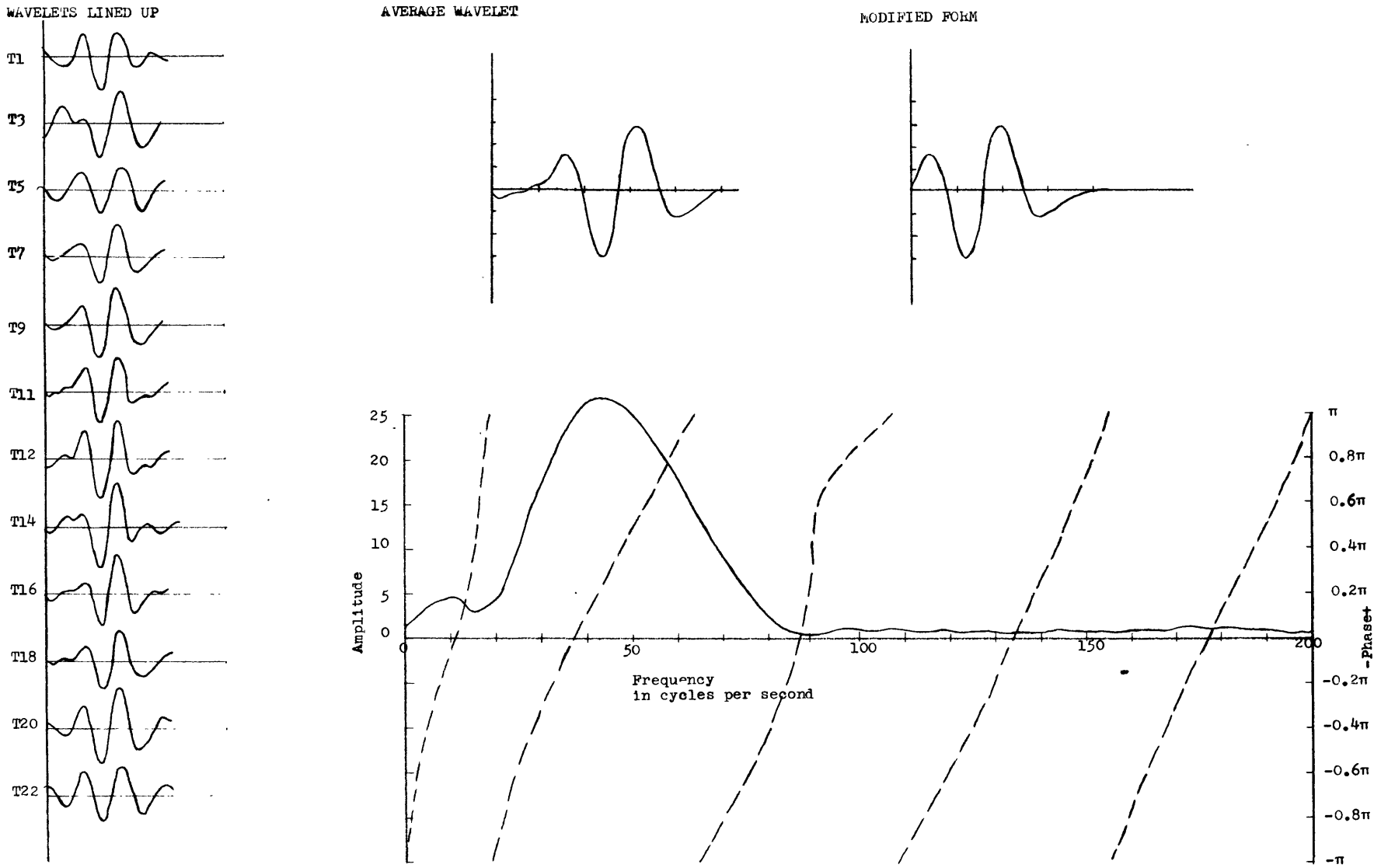

Fig. 13 The average wavelet from 7.19 and its spectral characteristics

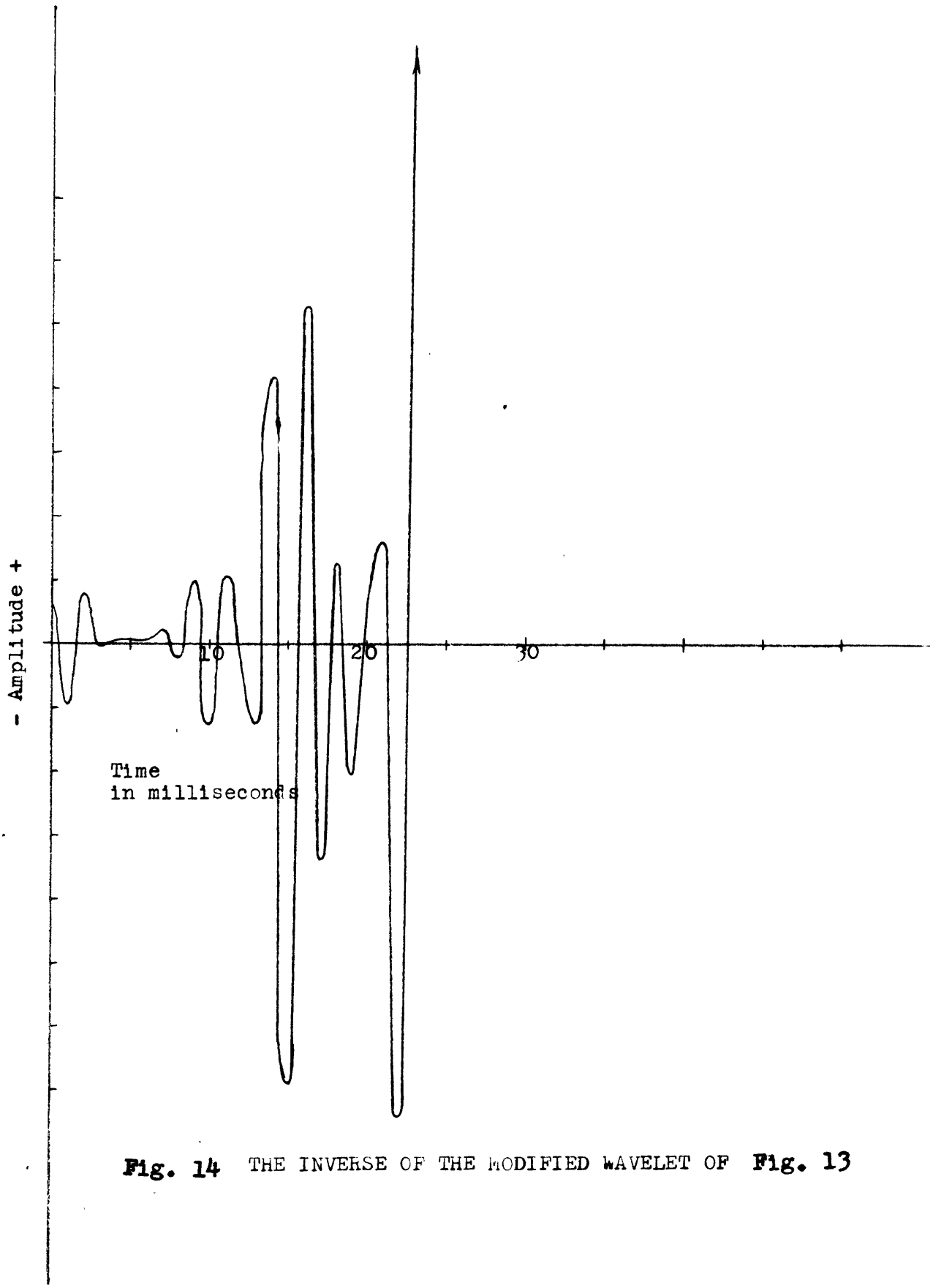

Fig. 14 THE INVERSE OF THE MODIFIED WAVELET OF **Fig. 13**

The first nine terms seem all that we should really employ in forming an inverse operator. This operator, although of very limited use, is nevertheless good enough to separate the first wavelet in the noiseless case from another waveform. In order to check this the wavelet complex occurring around 1.07 seconds on 7.19 was averaged in the same manner as was the original wavelet. This complex was added on to the first wavelet after a time lag of four spacings (10 milliseconds) and this new complex was then convolved with the first nine terms of our inverse. In this noiseless case the onset of the two events was quite clear (see Fig. 15). This limiting condition of a noiseless system in which we are only able to discern between events occurring within 20 milliseconds is quite restricting. As we notice when we convolve our nine term operator with some of the actual traces from 7.19 the noise in the actual cases tends to obscure any spiking (Fig. 16). Our inverse approach is applicable however in discerning the onset of a second event shortly after the known onset of a known waveform in a relatively noiseless system. These conditions are quite restrictive and we are therefore left to search for another approach.

We were next led to attempting to fit a Ricker wavelet to our wavelet in the hope that this would be suitable means of creating an inverse operator. Due to the configuration of our waveform which we previously discussed the closest fit was to $V(\infty)$. Convolution of the inverse obtained from our modified $V(\infty)$ and the first modified wavelet from 7.19 produced diverging terms with no recognizable spike. This method was then dropped.

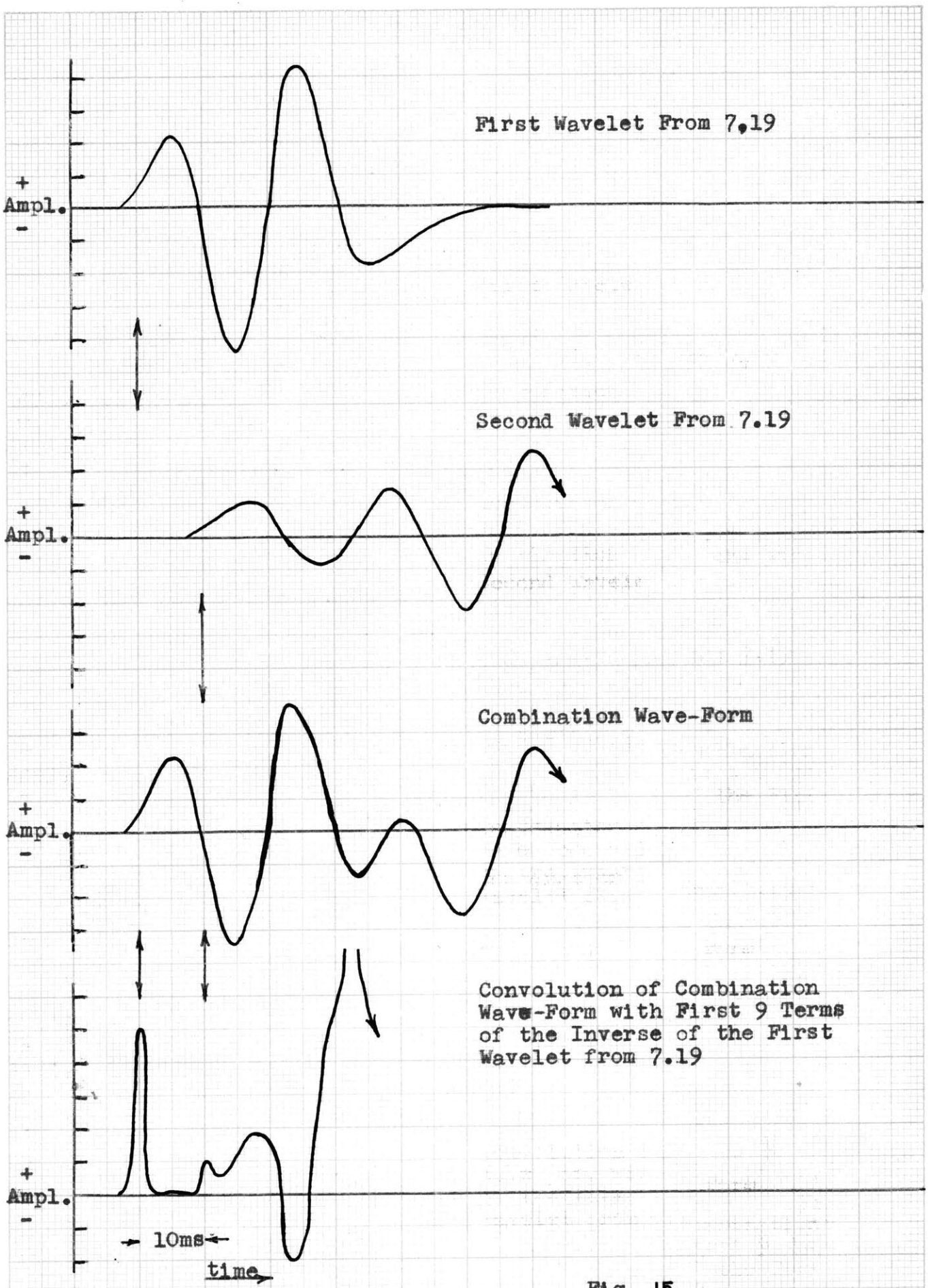
First Wavelet From 7.19
+
Ampl.
-
Second Wavelet From 7.19
+
Ampl.
-
Combination Wave-Form
+
Ampl.
-
Convolution of Combination Wave-Form with First 9 Terms of the Inverse of the First Wavelet from 7.19
+
Ampl.
-
10ms
time

Fig. 15

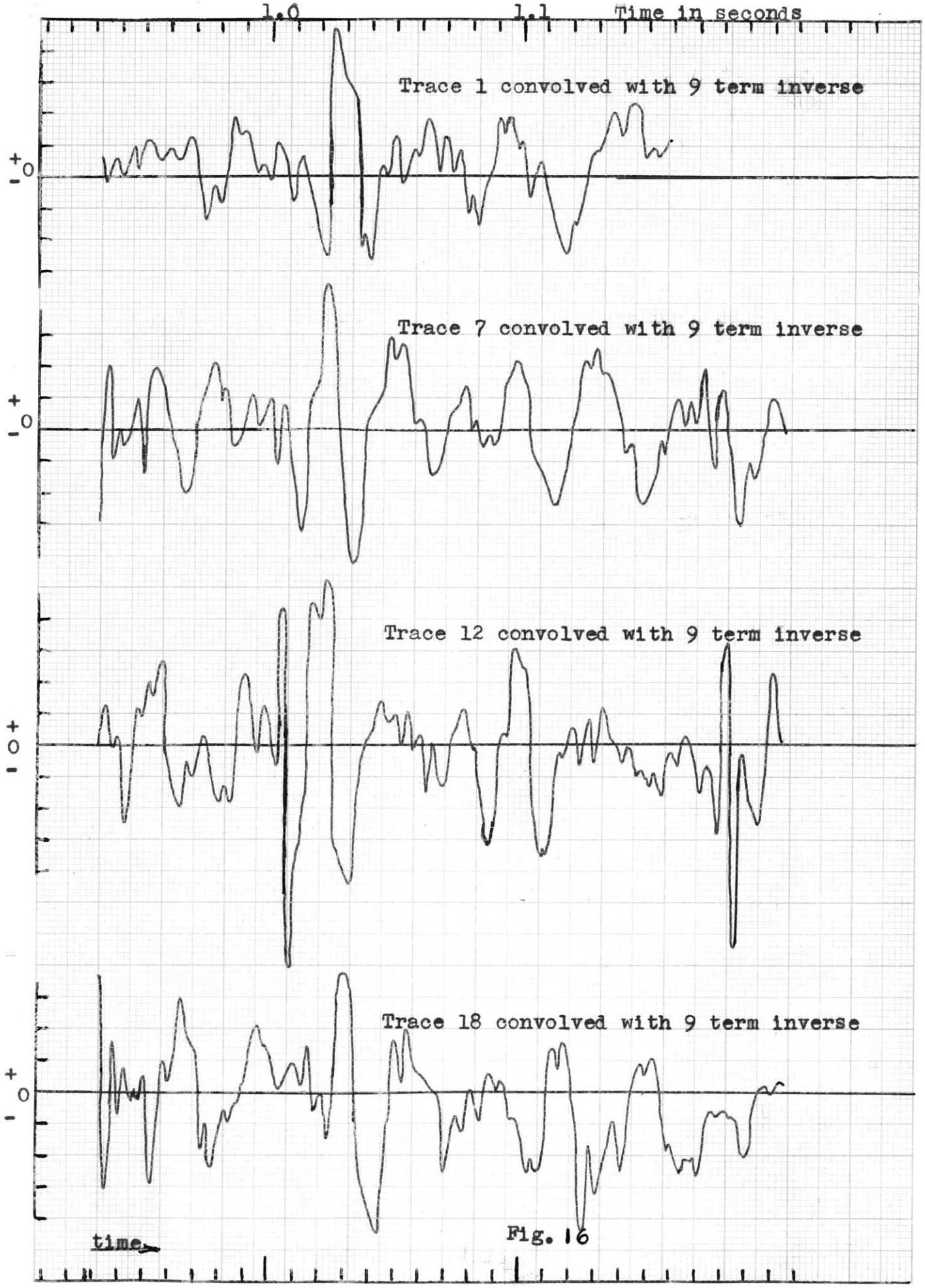
1.0
1.1
Time in seconds
Trace 1 convolved with 9 term inverse
+
0
-
Trace 7 convolved with 9 term inverse
+
0
-
Trace 12 convolved with 9 term inverse
+
0
-
Trace 18 convolved with 9 term inverse
+
0
-
time

Fig. 16

A STUDY OF THE RESOLUTION OF A SYMMETRIC OPERATOR CHOSEN TO PRODUCE CONTRACTION OF A SPECIFIC WAVEFORM

In the ideal case in which we are concerned with a stable wavelet (i.e. having a stable inverse) it is seen that our convolution process will produce a single spike which has a white light amplitude spectrum. It was hoped therefore, that we might be able to produce contraction, although surely not a single spike, if we convolved experimental wavelets with the damped series which are the cosine transforms (unfolded to produce a symmetric operator) of the reciprocals of the amplitude spectrums for the original waveforms. This convolution would have as its output a series which would have a white light spectrum and which it was hoped would be a close approximation to a spike.

The reciprocal of the amplitude spectrum was, therefore, computed for both the sharp-front wavelet (i.e. initial value was quite large - as used in finding an inverse) modified from the averaged wavelet from Record 7.19 and a modification of the same wavelet smoothed so as to have gradually increasing amplitudes before its first positive maximum (compare wavelets on Figs. 19 and 20). The cosine transforms for both of these reciprocal amplitude spectrums were computed and are also shown on Figs. 17 and 18. In order to investigate the contraction properties various lengths of these symmetric operators were then convolved with the smoothed and sharp-front wavelet. In Fig. 19 the symmetric operator formed from the sharp-front wavelet to 49, 25 and 15 terms was convolved with the sharp-front wavelet. These results show very good spiking for all three lengths of the operator with similar forms and amplitudes in each case. The dependence on operator length was evident in Fig. 20 where we convolved 49, 25 and 15 terms respectively of the symmetric operator(formed from the smoothed wavelet) and the smoothed wavelet itself. Here we notice that the 25 term and 49 term operators

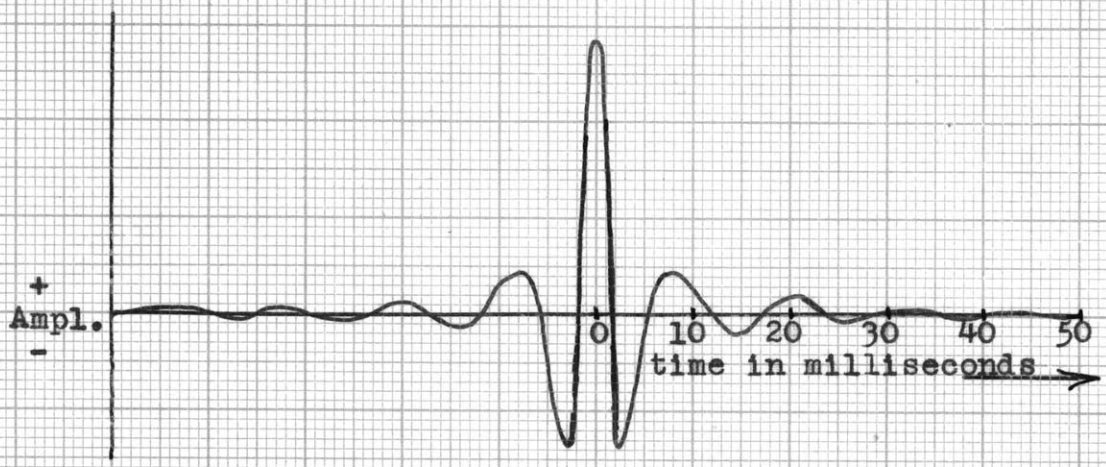

SYMMETRIC OPERATOR FOR SMOOTHED WAVELET FROM 7.19

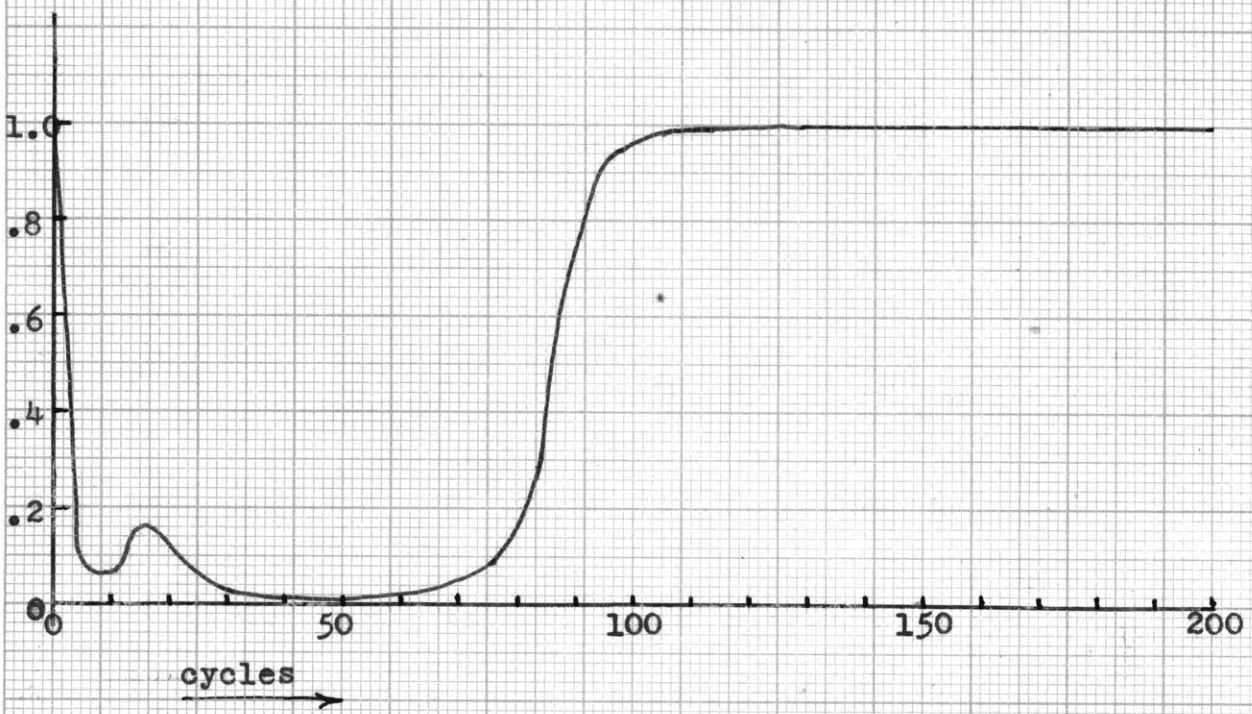

RECIPROCAL OF AMPLITUDE SPECTRUM OF SMOOTHED WAVELET FROM 7.19

Fig. 17

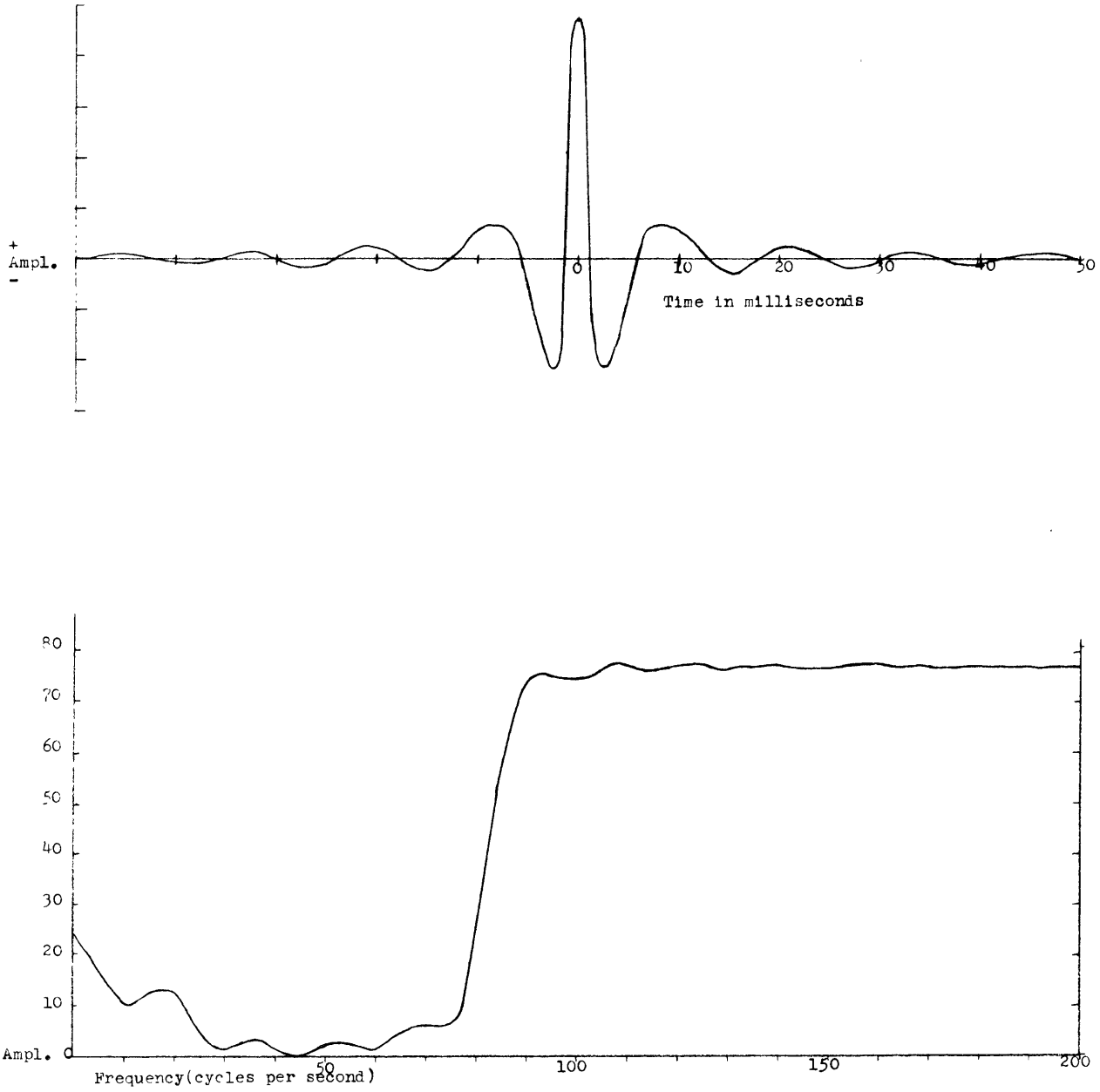

Fig. 18 **Symmetric operator and its amplitude characteristics obtained from cosine transform of reciprocal of amplitude characteristic of Sharp-Front Wavelet**

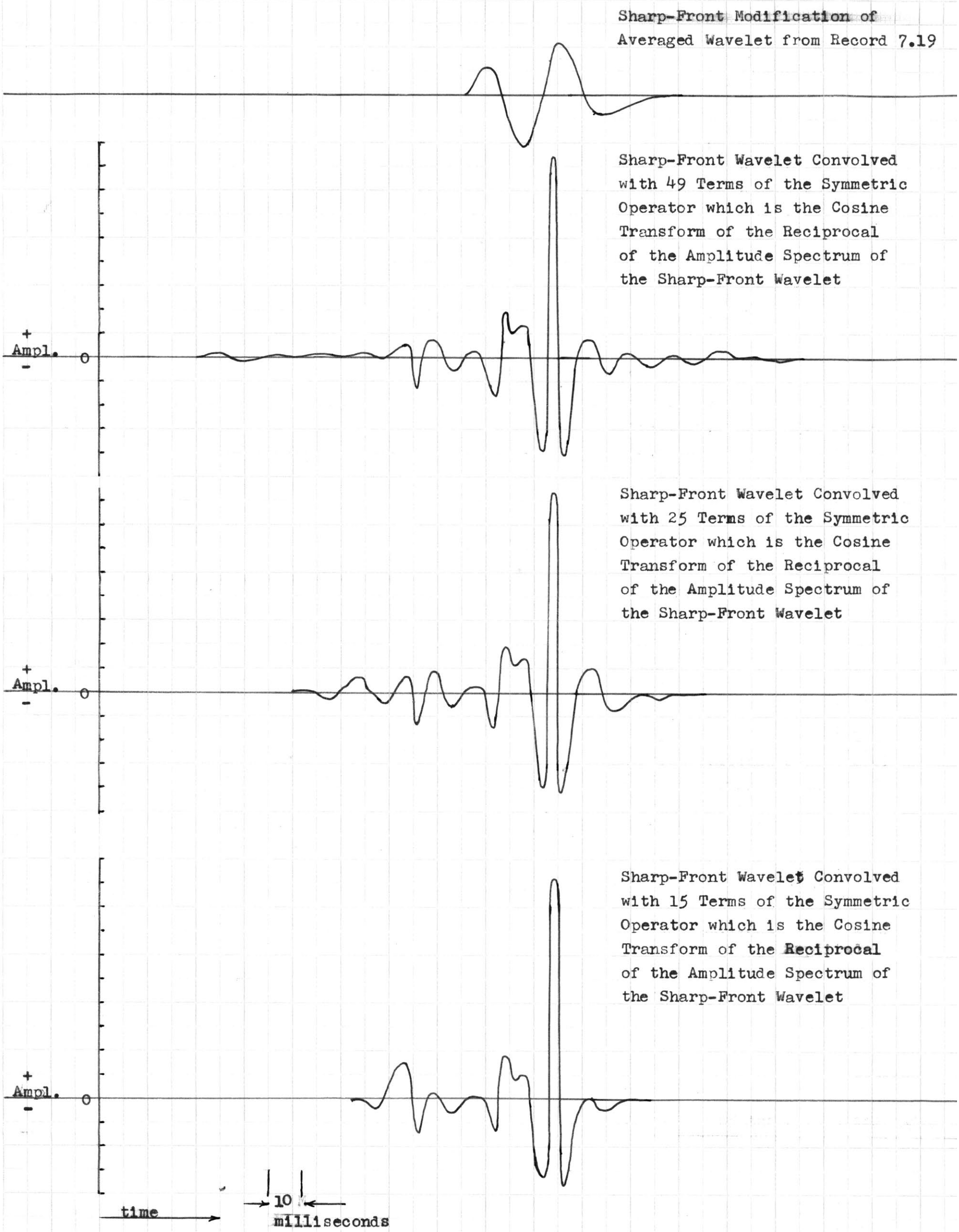
Sharp-Front Modification of
Averaged Wavelet from Record 7.19
Sharp-Front Wavelet Convolved
with 49 Terms of the Symmetric
Operator which is the Cosine
Transform of the Reciprocal
of the Amplitude Spectrum of
the Sharp-Front Wavelet
+
Ampl.
-
0
Sharp-Front Wavelet Convolved
with 25 Terms of the Symmetric
Operator which is the Cosine
Transform of the Reciprocal
of the Amplitude Spectrum of
the Sharp-Front Wavelet
+
Ampl.
-
0
Sharp-Front Wavelet Convolved
with 15 Terms of the Symmetric
Operator which is the Cosine
Transform of the Reciprocal
of the Amplitude Spectrum of
the Sharp-Front Wavelet
+
Ampl.
-
0
time
10
milliseconds

Fig. 19

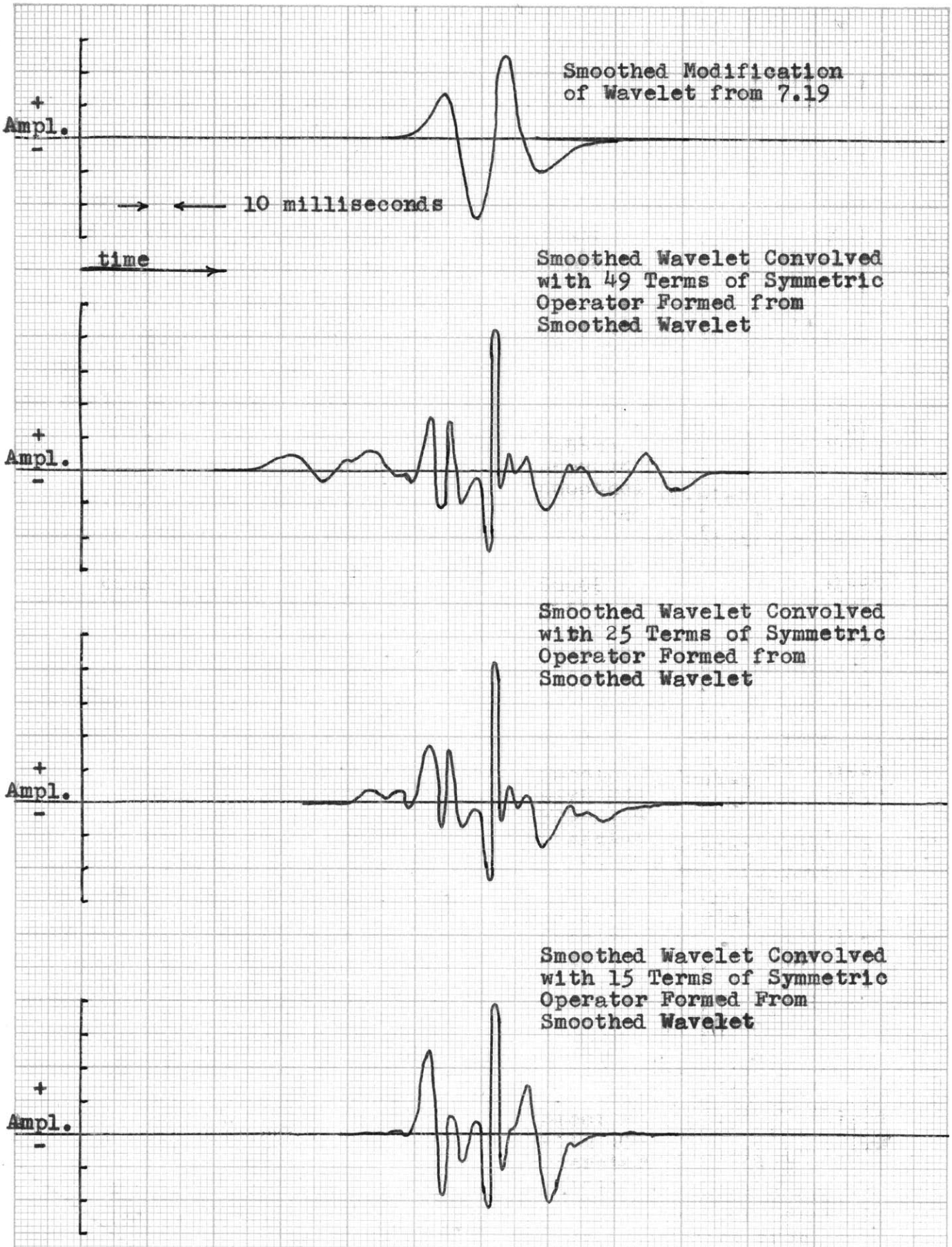
Smoothed Modification
of Wavelet from 7.19
+
Ampl.
-
10 milliseconds
time
Smoothed Wavelet Convolved
with 49 Terms of Symmetric
Operator Formed from
Smoothed Wavelet
+
Ampl.
-
Smoothed Wavelet Convolved
with 25 Terms of Symmetric
Operator Formed from
Smoothed Wavelet
+
Ampl.
-
Smoothed Wavelet Convolved
with 15 Terms of Symmetric
Operator Formed From
Smoothed Wavelet
+
Ampl.
-

Fig. 20

produce relatively low leading and trailing amplitudes in comparison with the results of the 15 term convolution. The leading and trailing amplitudes for the convolutions in these two experiments were small compared with the amplitude found with the 25 and 15 term convolutions shown in Fig. 21 where the symmetric operator developed from the sharp-front wavelet was convolved with the smoothed wavelet. In this experiment the 49 term operator produced a usable spike despite the variation in waveform. This seems to indicate that this method is at least less sensitive to small variations in wavelet shape than our inverse approach.

It was hoped that we might be able to decrease the leading and trailing amplitudes by smoothing our symmetric operator. A method of Cesaro sums was used on our operator formed from the sharp-front wavelet giving zero initial and terminal values and weighting each of the ordinate values linearly from these zero extremes to the maximum at the point of symmetry. The convolution of this revised symmetric operator (taken to 49, 25 and 15 terms) with the smoothed wavelet resulted in a drastic reduction in contraction as is shown in Fig. 22. It was concluded that the amplitudes of leading and trailing terms of the operator could not be diminished by this process without a marked loss in contraction and this variation was dropped.

It was noticed that the symmetric operator formed from the sharp-front wavelet to 49 terms produced a spike when convolved with the smoothed wavelet and that the symmetric operator formed from the smoothed wavelet to 25 and 49 terms produced similar results when convolved with the smoothed wavelet. Now inasmuch as a smoothed wavelet seems to be more physical than one with a sharp-front - and since the convolutions from the latter's operator seem to be somewhat better - it was decided that the 25 term operator from the smoothed wavelet and the 49 term operator from the sharp-front wavelet would be used in further experiments concerning this method.

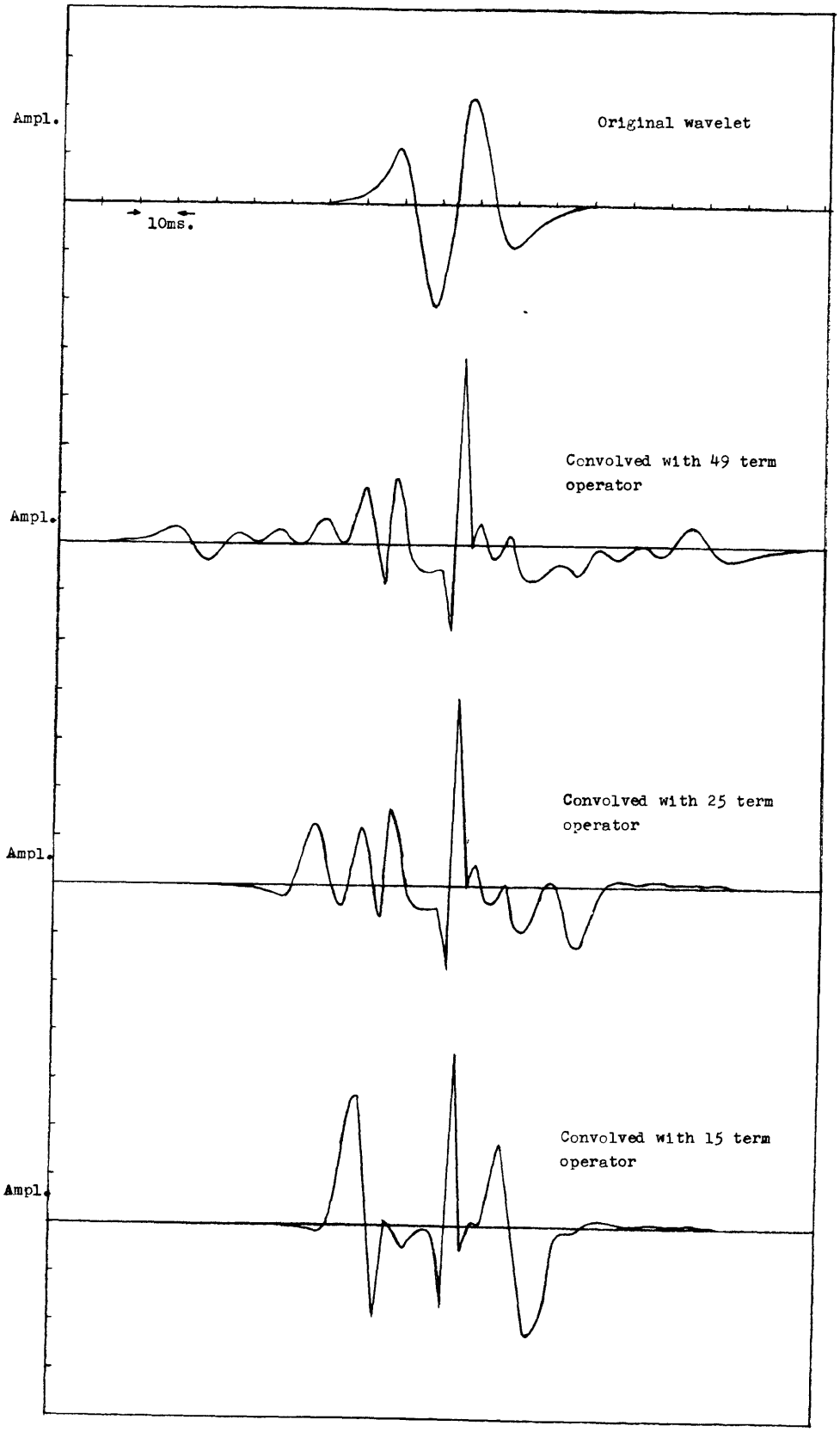

Fig. 21 Convolutions of Symmetric Operator Formed from Smoothed Wavelet with Sharp-Front Wavelet

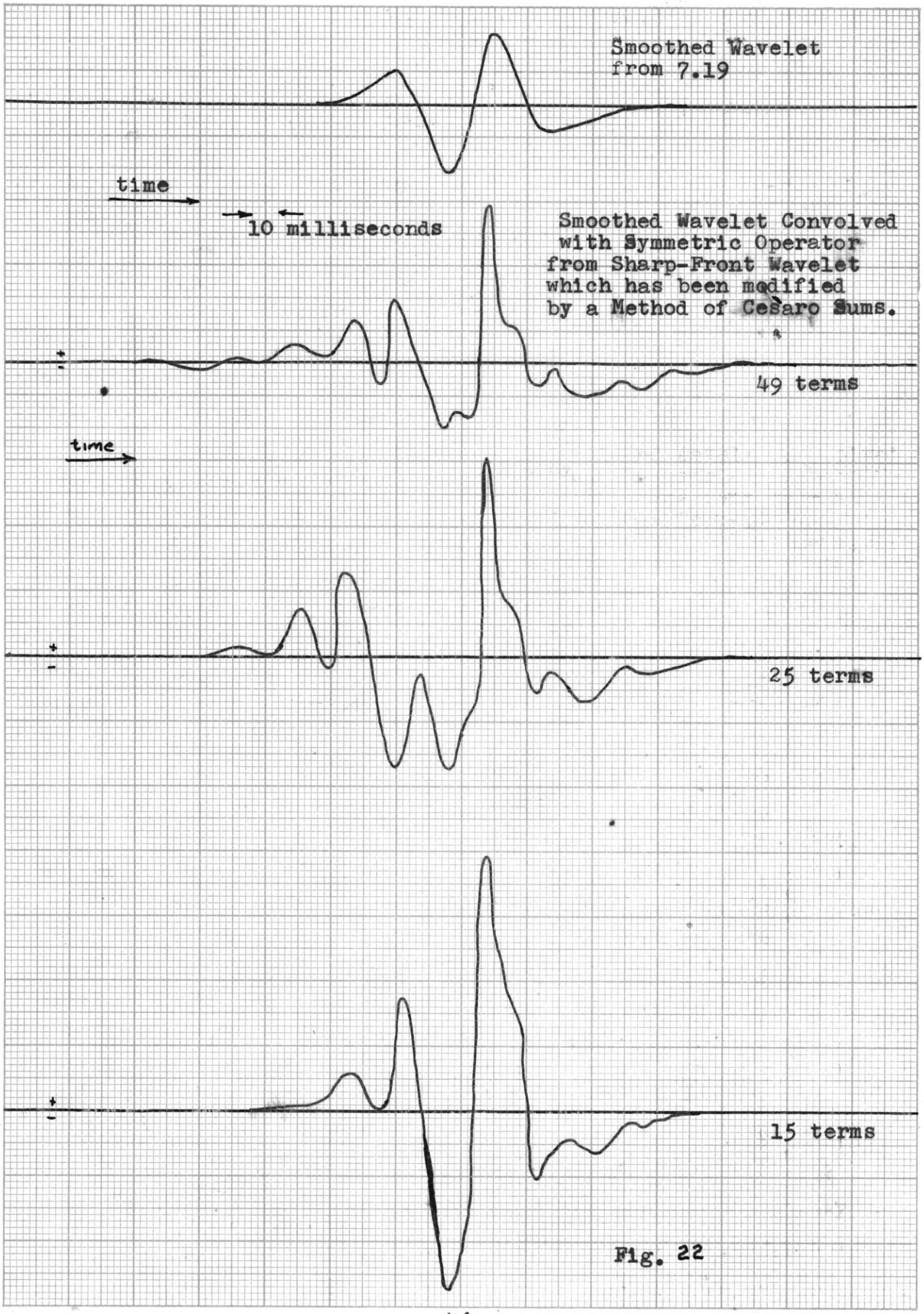
Smoothed Wavelet
from 7.19
time
10 milliseconds
Smoothed Wavelet Convolved
with Symmetric Operator
from Sharp-Front Wavelet
which has been modified
by a Method of Cesaro Sums.
49 terms
time
25 terms
15 terms

Fig. 22

In an attempt to find how our contractor operators would behave on an actual seismic record we convolved 25 terms of the symmetric operator formed from the smoothed wavelet and 49 terms of the symmetric operator formed from the sharp-front wavelet with alternate traces from Record 7.19 over the interval from 0.91 seconds to 1.16 seconds (refer to Fig. 12). These results are shown in Figs. 23 and 24 respectively, and are both encouraging and discouraging. The results are noticed to be very similar and in this experiment there seems little advantage of one operator over the other. It is seen that the first event or reflection is evident when looking at the filtered record section as a whole, but that the second event, expected at about 1.07 seconds, is obscured. This may be attributed to the fact that our second waveform on Record 7.19 is a complex and is probably much different from our first wavelet (see Fig. 15). In practice we might then find the cosine transform of the reciprocal of the amplitude spectrum for the second waveform and use it as an operator over the same interval in order to pick out the second event. Carrying out these two independent operations on the complex on Record 7.16 we might then expect to find the onset times of the two events.

Another note of interest in connection with Figs. 23 and 24 is that the spiking appears to die out on certain traces where there was an identifiable waveform on the original records. This suggests again the possibility of phasing and noise effects.

In order to study the effects of phasing, ordinate values of the smoothed wavelet were interpolated for each 1/8 th spacing (original time interval = 2.5 milliseconds, here we interpolated an ordinate for every $\frac{2.5}{8}$ milliseconds interval). The convolutions were then performed of 25 terms of the symmetric operator formed from the smoothed wavelet and 49 terms of the symmetric operator formed from the sharp-front wavelet with the smoothed wavelet with ordiante values corresponding to a shift of 1/4, 1/2, and 3/4 data spacings (by a similar arrangement to that shown in Fig. 10). These results are shown respectively

A PORTION OF RECORD 7.19 FILTERED BY THE SYMMETRIC OPERATOR FORMED FROM THE SMOOTHED WAVELET

Fig. 23

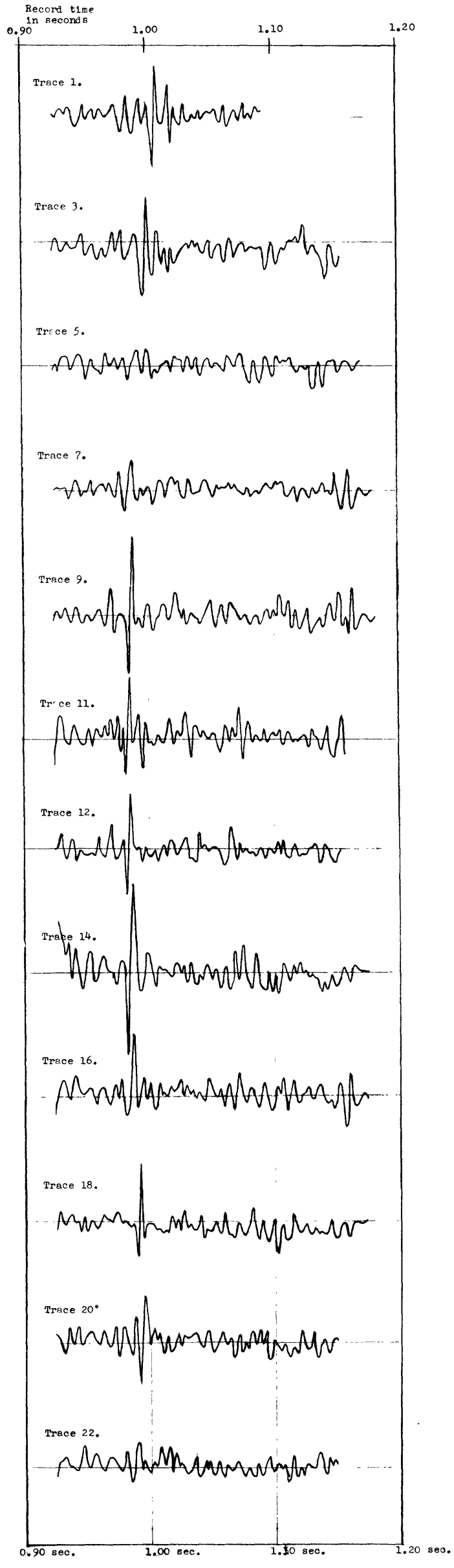

Fig. 24 A portion of record 7.19 filtered by symmetric operator formed from sharp-front wavelet

in Figs. 25 and 26. Here we notice that the spacing and relative breadth of our waveform are very critical. As expected, the worst resolution was produced with the half shift where the convolution in both cases produced two diminished spikes instead of the single event which was produced in the convolutions where there was no shift. It would be very difficult to tie down the onset of the first event let alone pick out the onset of the second overlapping event on any single trace if the onset of the first signal satisfied this worst case. With the present phase-dependent convolutions we must depend on the ensemble of convolutions across the record for resolution, weighting more strongly the results of the in-phase traces.

It was hoped that we might eliminate the phasing effects by decreasing our data spacing and therefore another phase test was set up. The values of our symmetric operators, the 25 term operator formed from the smoothed wavelet and the 49 term operator formed from the sharp-front wavelet, were interpolated for half spacing. These new operators were then convolved with the smoothed wavelet with 1/2 spacing shifted 1/8, 1/4, and 3/8 of the original 2.5 millisecond spacing. The results are shown in Figs. 27 and 28 and, as the results are similar for all members of the two sets, we can conclude that finer spacing will solve the phasing problem. However, it is also noticed that there has been a decided decrease in the contraction. This may quite probably be due to the inaccuracies of the interpolation used to form the symmetric operators for the half spacing and hence to the difference of the interpolated values from actual values which could be calculated exactly. It is felt that the 1/2 spaced operators will be more sensitive to changes in wave shape but that with a more accurate computation of the symmetric operator the resolution should be almost as good for any shift with 1 /2 spacing as it is for the exact fit with regular spacing. Mathematically it can be shown that the above relationship holds

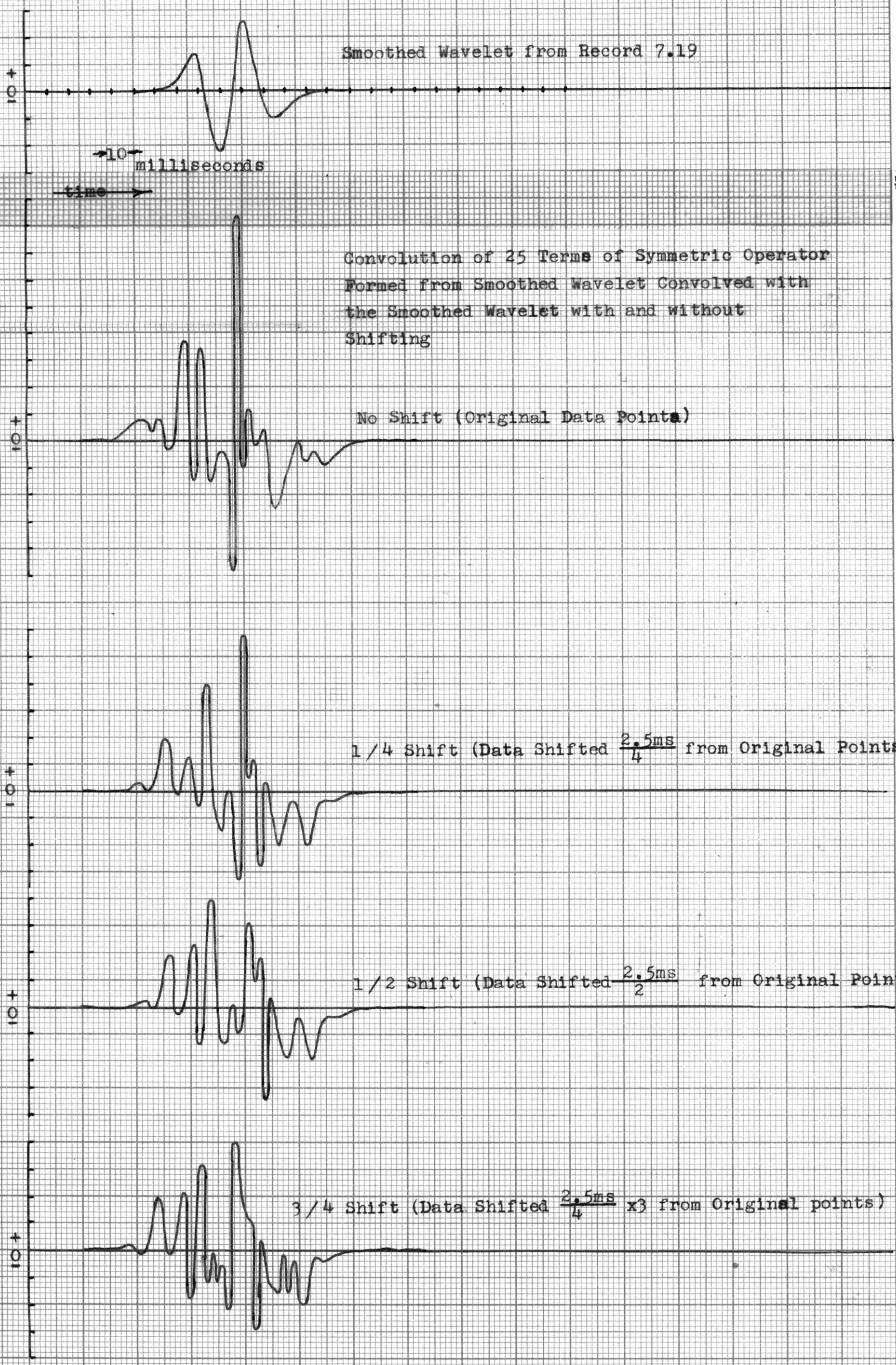

PHASE TEST --SMOOTHED WAVELET CONVOLVED WITH SYMMETRIC OPERATOR FROM SMOOTHED WAVELET

Fig. 25

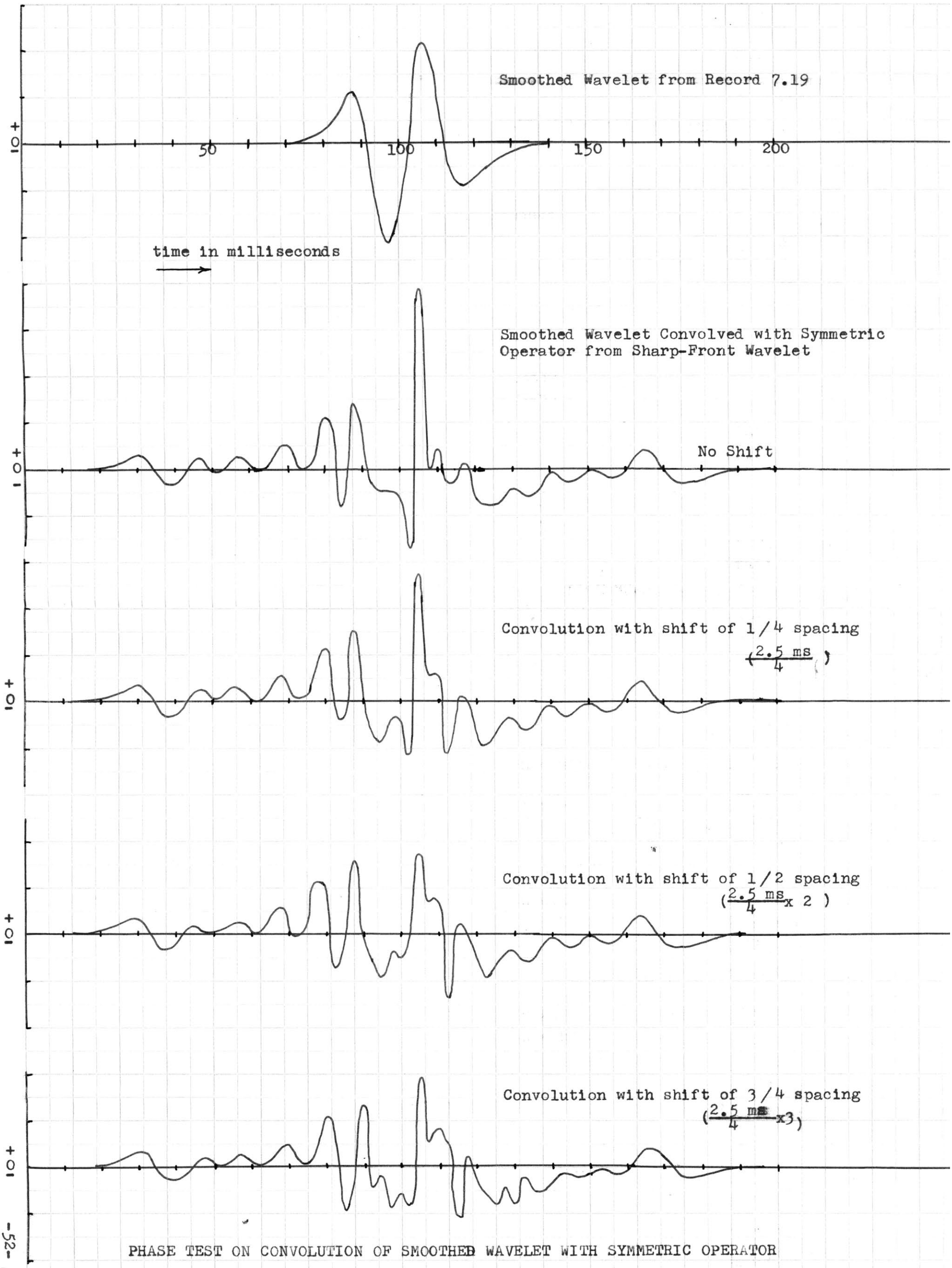

PHASE TEST ON CONVOLUTION OF SMOOTHED WAVELET WITH SYMMETRIC OPERATOR FROM SHARP-FRONT WAVELET (49 terms)

Fig. 26

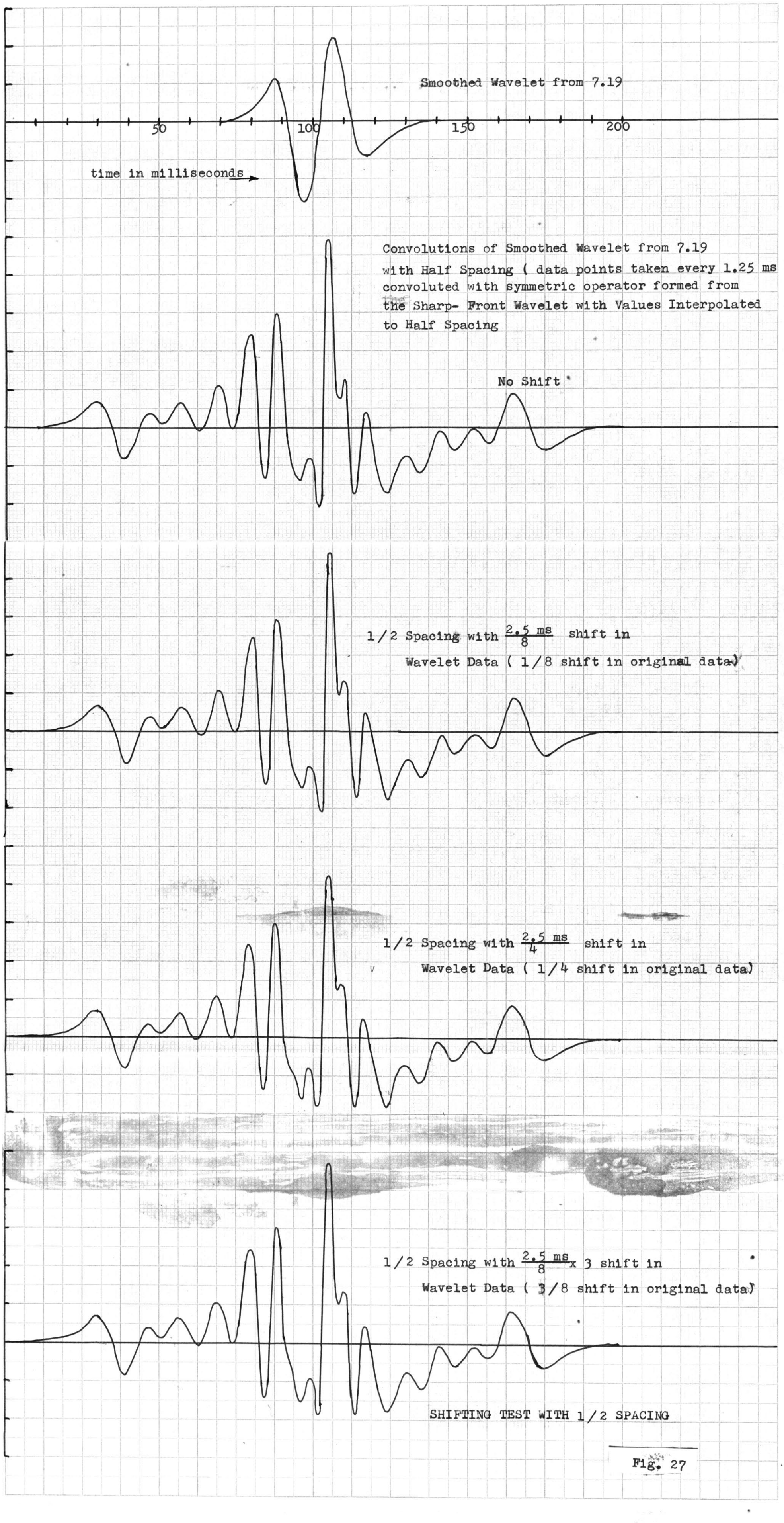

SHIFTING TEST WITH 1/2 SPACING

Fig. 27

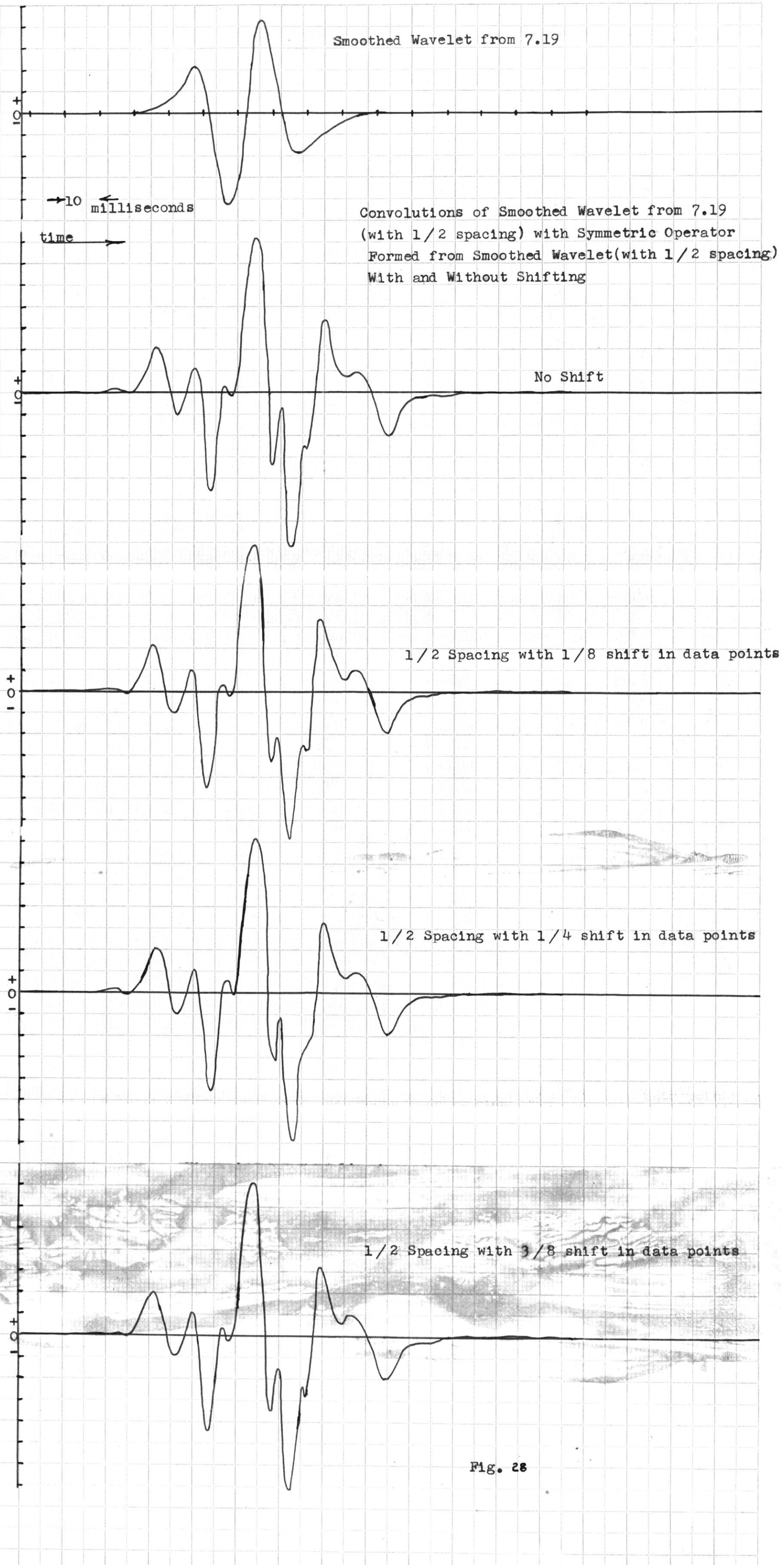
Smoothed Wavelet from 7.19
+
0
-
→10 ← milliseconds
time →
Convolutions of Smoothed Wavelet from 7.19
(with 1/2 spacing) with Symmetric Operator
Formed from Smoothed Wavelet(with 1/2 spacing)
With and Without Shifting
No Shift
1/2 Spacing with 1/8 shift in data points
1/2 Spacing with 1/4 shift in data points
1/2 Spacing with 3/8 shift in data points

Fig. 28

and is only in the nature of our data handling that we have failed to produce the desired contraction. For completeness we also convolved the smoothed wavelet and the symmetric operator from the sharp-front wavelet to 1/4 spacing (Fig. 29). These results show a larger decrease in the contraction than did the experiments at 1/2 spacing and further indicate that our interpolations were not yielding accurate ordinate values.

Further investigation is proposed inasmuch as there is a good possibility that, with closer calculation of the cosine transform of the reciprocal of the amplitude spectrum for the half spaced wavelet data, we can produce an operator which will have little or no phase dependence and which will contract the wavelets. If, due to the nature of our data, we are unable to obtain an operator which has the above properties and is also fairly insensitive to small changes in wavelet shape, our method may still be of some value. Looking at an ensemble of seismic traces operated on by one of the symmetric operators such as in Fig. 23 or 24 the contraction obtained with using data of the original type (spacing = 2.5 milliseconds) may be enough to pick out the first event. Subsequent operation with an operator designed to contract a second event may likewise indicate the time of occurrence of that event. Adding the results found in both operations and taking into account the overall effects we may be able to obtain the desired information as to the boundaries of our thinning bed.

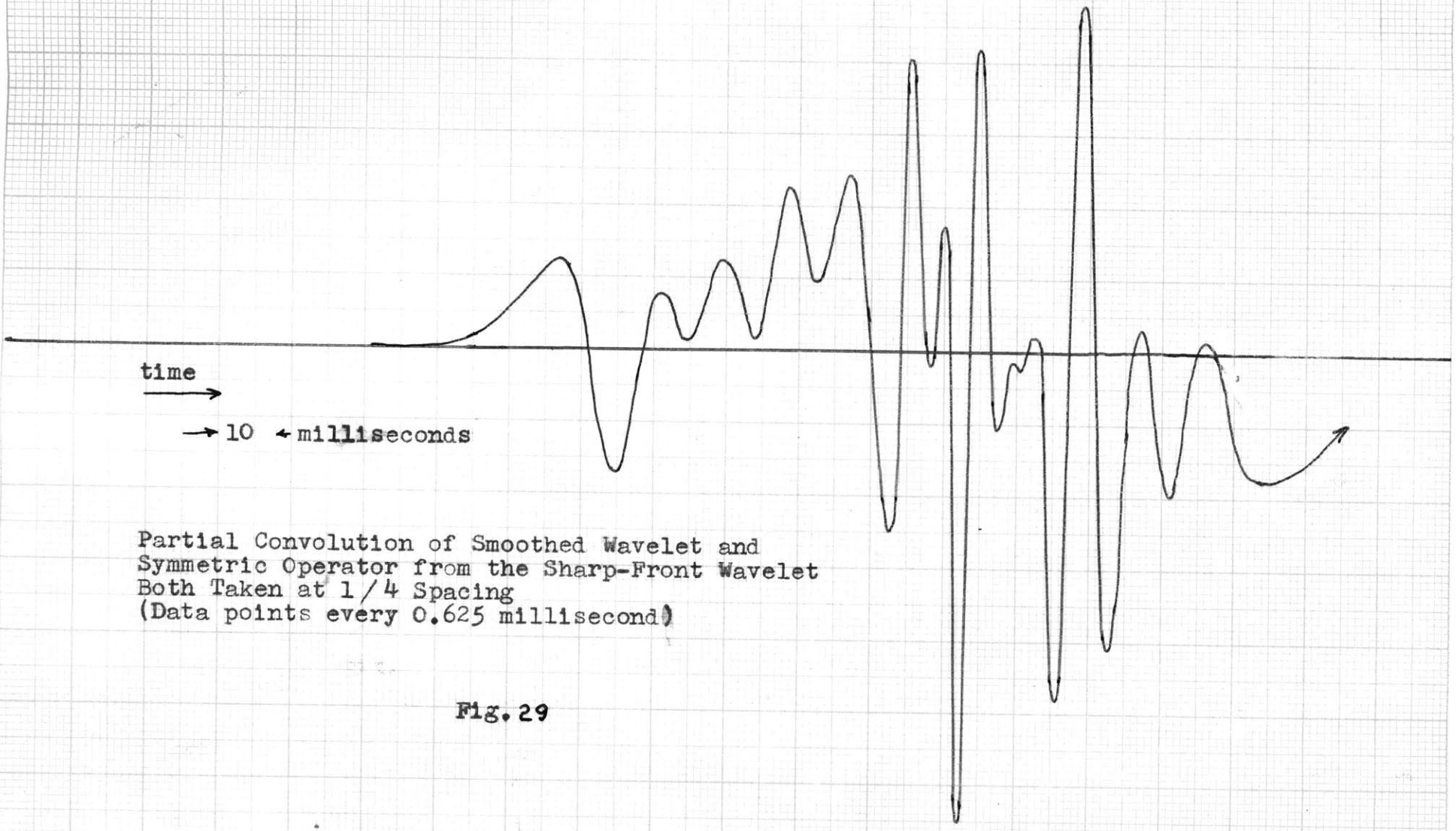

Partial Convolution of Smoothed Wavelet and
Symmetric Operator from the Sharp-Front Wavelet
Both Taken at 1/4 Spacing
(Data points every 0.625 millisecond)

Fig. 29

LEAST SQUARES METHOD OF RESOLVING OVERLAPPING SEISMIC SIGNALS

The above approaches to solving our general problem seem to have limitations and therefore a method of least squares fitting is also proposed. This method is computationally much more involved than any plan set up thus far in this paper. It is therefore suggested that the method, mathematically set up below, be programed for a digital computer and tested. If the resolving power is good enough it is then suggested that, economics having been weighed, special purpose analog equipment be built to do the same work. This analog system would of course run large amounts of data much more economically than a digital machine to the accuracies required.

A Least Squares Fitting Method of Resolving Overlapping Seismic Signals

In applying a method of least squares we first will describe the procedure using functional notation and then will develop the discrete form which we will have to deal with in an analysis by digital means.

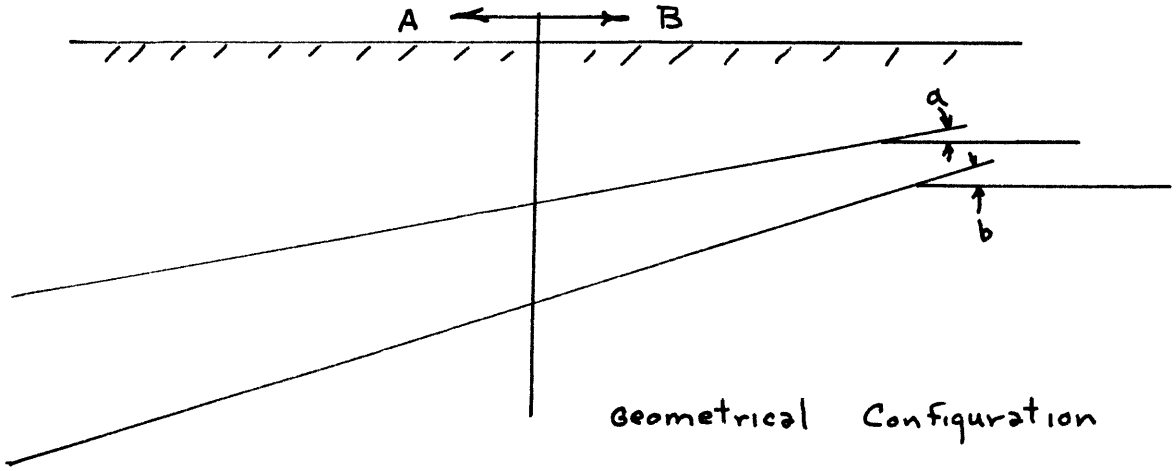

Fig. 30

We will in general be interested in extending the resolution of reflections from two horizons from an area A where these two events are distinguishable on seismic records to an area B where the reflectors are close enough together that their waveforms overlap and where one or both of their onsets can not be distinguished. (see Fig. 30.) We further assume that in area A the two events are represented by the onset of two distinct waveforms W(t) and U(t) respectively. These two events may be determined by an averaging process over records in area A, (See Fig. 31) requiring that similar filters are used, it is assumed that the average wavelet representing the reflection of a horizon in area A will remain constant in amplitude and duration for the same reflector in area B. This is of course a first approximation which might be relaxed later if more information were available.

Our two averaged waveforms W(t) and U(t) can be expressed

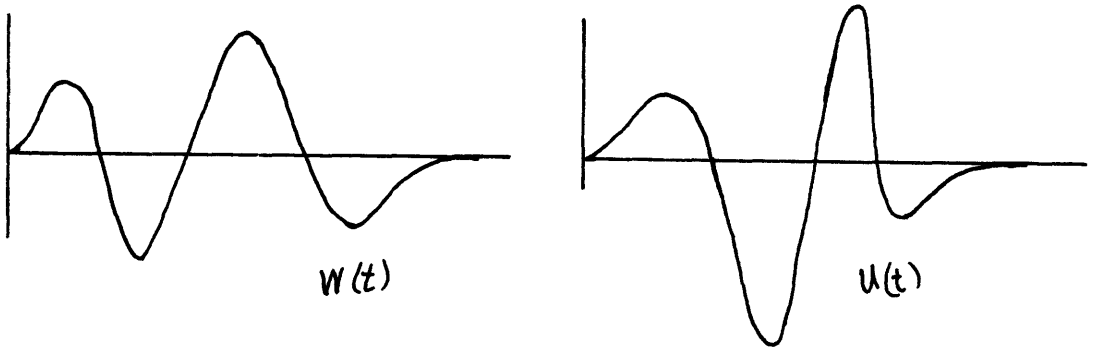

Fig. 31

as distinct time functions and their existence at set times after an arbitrary origin may be represented as W(t - x) and U(t - y)

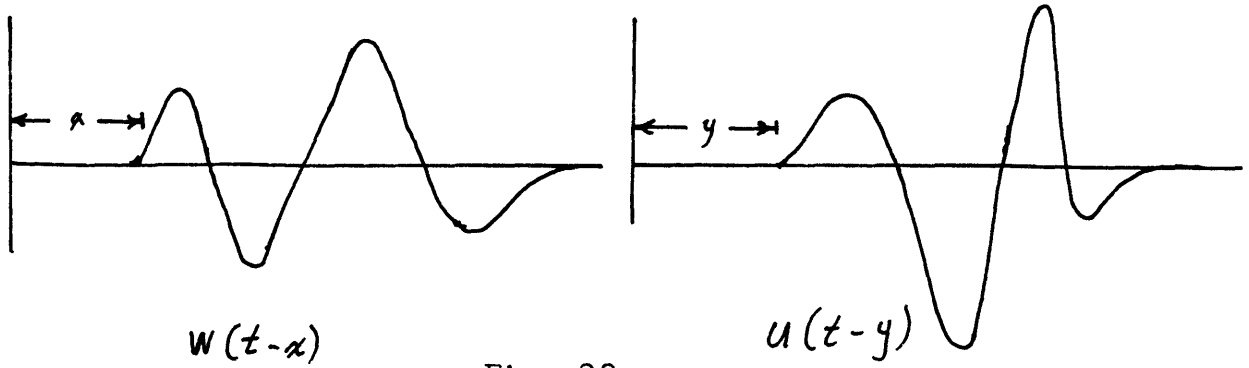

Fig. 32

Short Interval of Seismic Interest

As we are only interested in a short interval of the records in area B representing that period of time over which reflections from the two horizons are possible, we may set up a new time origin and limit encompassing this interval (Fig. 33).

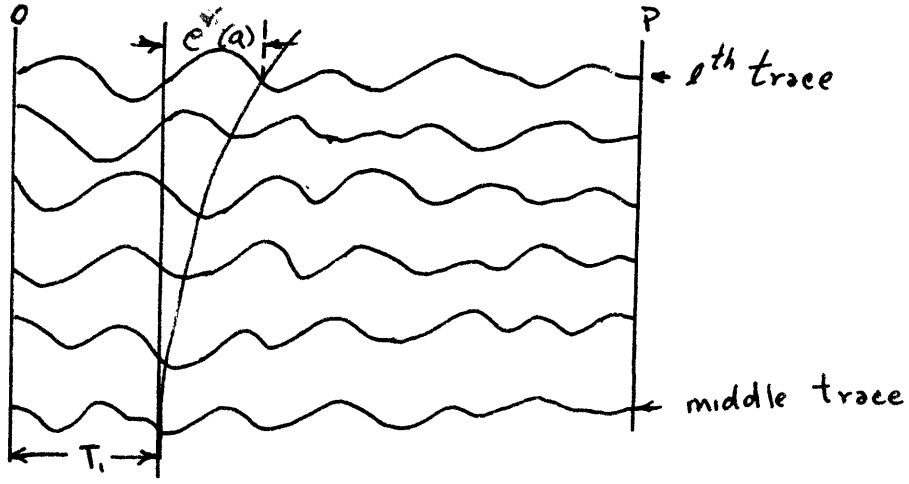

Fig. 33 Interval of Interest on Seismic Record

This restriction to a short seismic interval will allow us to deal with such parameters as velocities, normal move-out, and associated the geometries as constants. This will simplify our computation greatly. Likewise we will later realize simplification if we can restrict ourselves to small angles of dip.

Functional Relationships in Interval of Interest

Over this short interval we can then express the contribution of the first wavelet W(t) on the ℓth trace as $W(t - T_1 - e^{\ell}(a))$. Where T_1 is its time of onset on the middle trace from the time origin O and $e^{\ell}(a)$ is the move-out time to the ℓth trace for an angle of dip of the first reflector (a). Here we see that e^{ℓ} is a known function of a for the ℓth trace. Likewise we may represent the component of the ℓth trace due to the second wavelet as $U(t - T_2 - d^{\ell}(b))$ where T_2 is again the onset time on the middle trace and

$d^{\ell}(b)$ is the move-out time associated with the ℓth trace and the angle of dip b. of the second bed.

The ℓth trace may now be represented from O to P as the time series $F^{\ell}(t) = N^{\ell}(t) + W(t - T_1 - e^{\ell}(a)) + u(t - T_2 - d^{\ell}(b))$ Here $N^{\ell}(t)$ represents the noise function from O to P

Let us define

$$f^{\ell}(t) = W(t - \tau_1 - e^{\ell}(\alpha)) + u(t - \tau_2 - d^{\ell}(\beta))$$

where τ_1, τ_2, α, β are arbitrary functions. Then if the noise function $N^{\ell}(t)$ is uncorrelated with

$$W(t - T_1 - e^{\ell}(a)) \text{ and } u(t - T_2 - d^{\ell}(b))$$

on the average we can set up an error function

$$E^2(\tau_1, \tau_2, \alpha, \beta) = \sum_{\ell} \int_0^P (F^{\ell}(t) - f^{\ell}(t))^2 \, dt$$

and expect to find a minimum as

$$\left.\begin{array}{l} \tau_1 \longrightarrow T_1 \\ \tau_2 \longrightarrow T_2 \\ \alpha \longrightarrow a \\ \beta \longrightarrow b \end{array}\right\} \text{simultaneously}$$

In practice there is of course no unique minimum and there will probably be several over the interval. If we restrict ourselves first to a certain range of α's and β's and to possibilities that $\tau_2 > \tau_1$ our field is somewhat simplified. Making a good guess as to τ_1, τ_2, α, and β from information available in area A will be our best aid to solution. Having found the error function for the values of our first guess we next the gradient of this error function and use it to determine a new set of variables. With this new set of variables a new error function is calculated and the procedure

is cycled until the variations reach a lower designated limit. The function E^2 is seen to be dependent on four independent variables and thus in finding the gradient E^2 we have the direction of steepest descent in four dimensions.

Discrete Notation

Using the same geometries we now proceed to setting up the problem in a discrete form. We may consider the ℓth trace from O to P to be represented by

$$F^{\ell}(t) \underset{\text{for } t=ih}{\approx} F_1^{\ell} \qquad 0 \leq ih \leq P \qquad h = \text{spacing}$$

We consider our geophone-shotpoint configuration to be an in line split-spread set up with 2M recorders each spaced a distance s apart all occurring on a horizontal plane (i.e. our data has been assumed corrected to a plane surface as in Fig. 34).

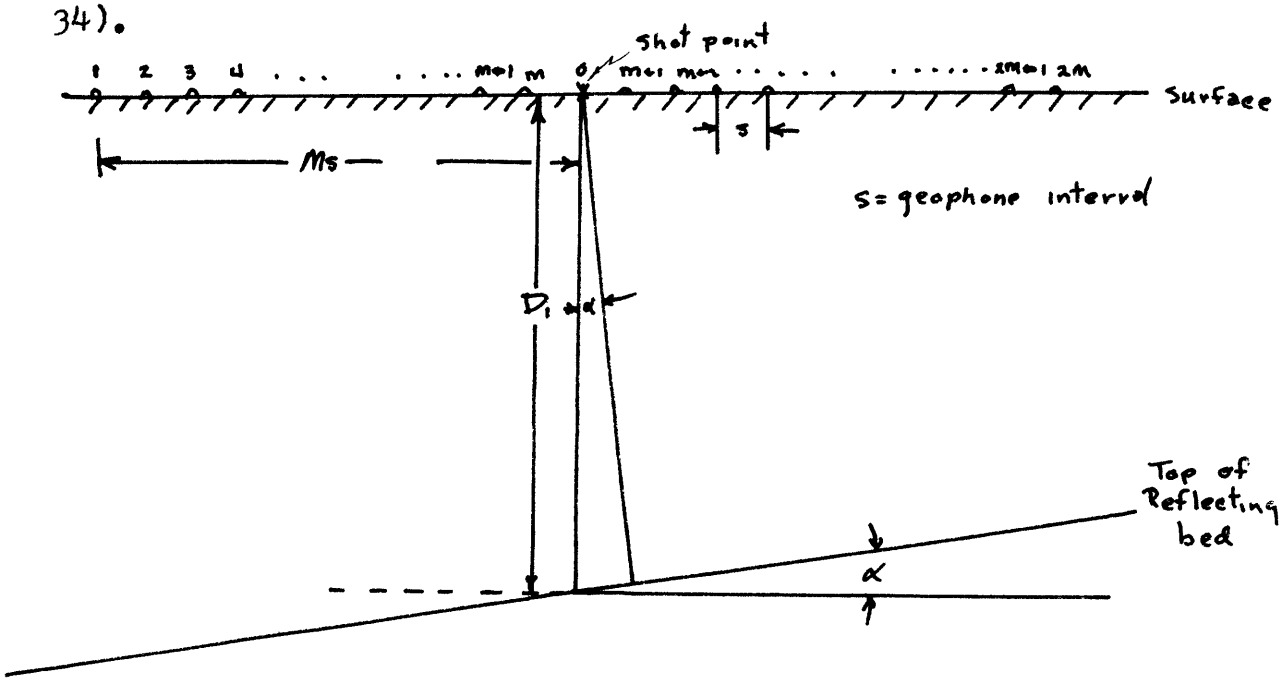

Fig. 34 Geometrical Configuration

τ_1 will now be $\tau_1 = \frac{2D_1}{\bar{V}\cos\alpha}$ where $\bar{V}$ is the average velocity considered for the interval O to P. The move-out time $e^{\ell}(\alpha)$ is somewhat more complicated. Considering the numbering of jugs from the down dip side to the up dip side separately (as shown in Section 4, Report 10b, MIT GAG)(2).

$$\left(\tau_1 + e^{\ell}(\alpha)\right)_L = \frac{(M-\ell)\left[\frac{Ms}{4D_1} + \cos\alpha \sin\alpha\right]Ms}{(M-1)\,\bar{V}\cos\alpha} \qquad \text{down dip}$$

$$\left(\tau_1 + e^{\ell}(\alpha)\right)_u = \frac{(\ell-M)Ms\left(\frac{Ms}{4D_1} - \cos\alpha \sin\alpha\right)}{(M-1)\,\bar{V}\cos\alpha} \qquad \text{up dip}$$

s=horizontal distance between geophones

subscripts L and u represent down dip and up dip respectively

From these expressions we can find the exact move-out times for any angle of dip and any trace number. For a first approximation, in order that we might simplify the computation, we assumed that our move-out times were linear functions of the trace numbers. That is to say, that the onset times of a given event on all the traces on one side of a split spread were assumed to lie on a straight line rather than along a curve (Fig. 35)

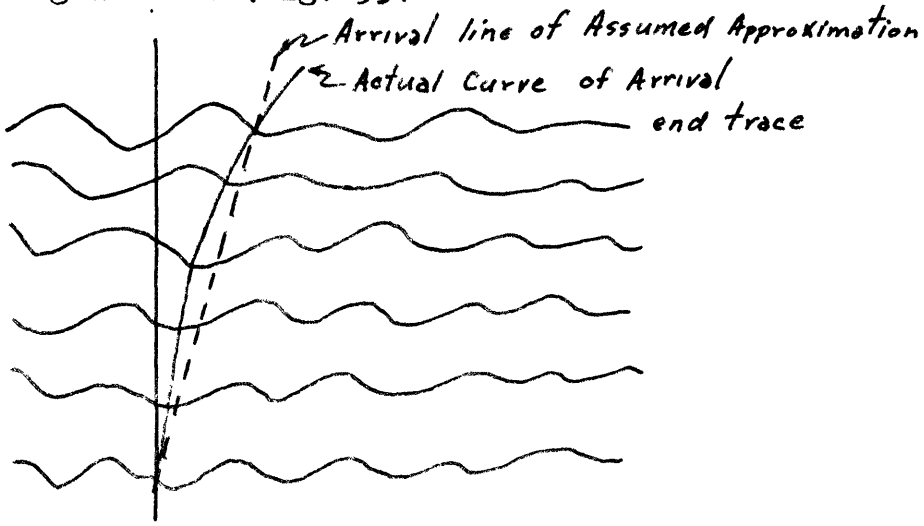

Fig. 35 Arrival of a Reflection Across a Seismogram

This assumption leads to relatively small errors (decreasing with depth) when compared with anomolous times of arrival due to small perturbations (MIT GAG Report 10b, Section 4 (2)).

$$\left(\tau_1 + e^{1}(\alpha)\right)_L = \left[\frac{M^2 s\left(\frac{Ms}{4D_1} + \cos\alpha \sin\alpha\right)}{(M-1)\,\bar{V}\cos\alpha}\right]$$

For the end traces

$$\left(\tau_1 + e^{2M}(\alpha)\right)_u = \left[\frac{M^2 s\left(\frac{Ms}{4D_1} - \cos\alpha \sin\alpha\right)}{(M-1)\,\bar{V}\cos\alpha}\right]$$

the middle trace $\left(\tau_1 + e^{m}(\alpha)\right) = \frac{2D_1}{\bar{V}\cos\alpha}$

an assumption which improves with depth.

The move-out times of our interval of interest

$$e^{1}(\alpha)_L = \frac{M^2 s\left(\frac{Ms}{4D_1} + \cos\alpha \sin\alpha\right) - 2D_1(M-1)}{(M-1)\,\bar{V}\cos\alpha}$$

$$e^{2M}(\alpha)_u = \frac{M^2 s\left(\frac{Ms}{4D_1} - \cos\alpha \sin\alpha\right) - 2D_1(M-1)}{(M-1)\,\bar{V}\cos\alpha}$$

$$e^{m}(\alpha) \approx 0$$

Now the move-out time per trace on the down dip side of the record will be

$$\epsilon(\alpha)_L = \left[\frac{M^2 s\left(\frac{Ms}{4D_1} + \cos\alpha \sin\alpha\right) - 2D_1(M-1)}{M(M-1)\,\bar{V}\cos\alpha}\right]$$

$$\epsilon(\alpha)_u = \left[\frac{M^2 s\left(\frac{Ms}{4D_1} - \cos\alpha \sin\alpha\right) - 2D_1(M-1)}{M(M-1)\,\bar{V}\cos\alpha}\right]$$

It is seen that these functions can be found for any angle if we assume a value for $\bar{V}$ and D. The step-out on the trace is now $(m - \ell) \Delta(\alpha)_L$ or $(\ell - m) \Delta(\alpha)_u$ depending on which side we are calculating. These move-out times when general will not produce integers and these quotients must be rounded off in order that the points of the digitalized traces will coincide. Otherwise a method of recalculating the amplitude values on the traces for each non-integer shift

$$\frac{(m - \ell) \Delta(\alpha)_L}{h} \quad \text{or} \quad \frac{(\ell - m) \Delta(\alpha)_u}{h}$$

would be necessary.

Likewise we find the move-out time per trace for our second wavelet

down dip

$$\delta(\beta)_L = \frac{M_s \left(\frac{M_s}{4D_2} + \cos\beta \sin\beta \right) - 2D_2 (M-1)}{(M-1)\, \bar{V} (\cos\beta)}$$

up dip

$$\delta(\beta)_u = \frac{M_s \left(\frac{M_s}{4D_2} - \cos\beta \sin\beta \right) - 2D_2 (M-1)}{(M-1)\, \bar{V} (\cos\beta)}$$

These move-out times may also be represented in discrete units of h. We shall consider these shift to be represented on the ℓth trace as

$$\frac{e^{\ell}(\alpha)_u}{h} \quad \text{and} \quad \frac{d^{\ell}(\beta)}{h}$$

where these functions will be rounded off to the nearest integers.

We now transfer our functional representations of our wavelets $W(t)$, $U(t)$, $W(t-x)$, and $U(t-y)$ into discrete notation.

$W(t) = W_i$ for $t = ih$ $\quad$ h = spacing interval

$U(t) = U_i$ for $t = ih$

$W(t-x) = W_{(i - \frac{x}{h})}$ for $t = ih$

$U(t-y) = U_{(i - \frac{y}{h})}$ for $t = ih$ (see figures 31 + 32)

Assume that W(t) is Q_1 units of h long and that U(t) is Q_2 units of h in duration.

$$\frac{x}{h} = \frac{\tau_1 + e^{\ell}(\alpha)_{\frac{u}{\ell}}}{h} \quad \text{and} \quad \frac{y}{h} = \frac{\tau_2 + d^{\ell}(\beta)_{\frac{u}{\ell}}}{h}$$

Then

$$W(t-x) = W\left(t - \tau_1 - e^{\ell}(\alpha)_{\frac{u}{\ell}}\right) = W_{i - \frac{\tau_1 + e^{\ell}(\alpha)_{\frac{u}{\ell}}}{h}} \quad \text{for } t = ih$$

and $W_{\left(i - \frac{\tau_1 + e^{\ell}(\alpha)_{\frac{u}{\ell}}}{h}\right)} = 0$ $\begin{cases} \text{for } i < \frac{\tau_1 + e^{\ell}(\alpha)_{\frac{u}{\ell}}}{h} \\ i > \frac{\tau_1 + e^{\ell}(\alpha)_{\frac{u}{\ell}}}{h} + Q_1 \end{cases}$

Likewise

$$U(t-y) = U\left(t - \tau_2 - d^{\ell}(\beta)_{\frac{u}{\ell}}\right) = U_{\left(i - \frac{\tau_2 + d^{\ell}(\beta)_{\frac{u}{\ell}}}{h}\right)} \quad \text{for } t = ih$$

and $U_{\left(i - \frac{\tau_2 + d^{\ell}(\beta)_{\frac{u}{\ell}}}{h}\right)} = 0$ $\begin{cases} \text{for } i < \frac{\tau_2 + d^{\ell}(\beta)_{\frac{u}{\ell}}}{h} \\ i > \frac{\tau_2 + d^{\ell}(\beta)_{\frac{u}{\ell}}}{h} + Q_2 \end{cases}$

We may now also set up $f^{\ell}(t)$ in discrete form.

for the ℓ^{th} trace

$$f^{\ell}(t) = f_i^{\ell} \qquad \text{for } t = ih$$

$$f^{\ell}(t) = W\left(t - \tau_1 - e^{\ell}_{(\alpha)}\right) + U\left(t - \tau_2 - d^{\ell}_{(\beta)}\right)$$

for $t = ih$

$$f^{\ell}_t = f_i^{\ell} = W_{\left(i - \frac{\tau_1 + e^{\ell}_{(\alpha)_u}}{h}\right)} + U_{i - \frac{\tau_2 + d^{\ell}_{(\beta)_u}}{h}}$$

and $f_i^{\ell} = 0$ $\begin{cases} i < \dfrac{\tau_1 + e^{\ell}_{(\alpha)_u}}{h} \\ i > \dfrac{\tau_2 + d^{\ell}_{(\beta)_u}}{h} + Q_2 \end{cases}$

$$\text{if } \frac{\tau_2 + d^{\ell}_{(\beta)_L}}{h} + Q_2 > \frac{\tau_1 + e^{\ell}_{(\alpha)_u}}{h} + Q_1$$

Having formed $f^{\ell}(t)$ we now proceed to find the error function.

$$E^2(\tau_1, \tau_2, \alpha, \beta) = \sum_{\ell=1}^{\ell=m} \sum_{t=0}^{t=P} \left(F_i^{\ell} - f_i^{\ell}\right)^2_L + \sum_{\ell=m}^{2m} \sum_{t=0}^{t=P} \left(F_i^{\ell} - f_i^{\ell}\right)^2_u$$

where subscripts u and L again denote up and down dip.

Steepest descent method applied to discrete data

Estimating τ_1, τ_2, α and β from what we observed in area A and using these values in the above error function a value of $E^2(\tau_1, \tau_2, \alpha \text{ and } \beta)$ is calculated. To improve this first estimate the gradient of the error function is taken at these values and we proceed along the gradient to our next estimate. This process is repeated until tolerances are met. In discrete notation we will proceed to this end by

means of variations. First we vary τ_1, by a small amount and calculate $E^2(\tau_1 + \Delta, \tau_2, \alpha, \alpha)$ holding the other functions at the original estimated values. Likewise we do the same thing for τ_2, α, and β increasing each of these by the same increment while holding the other variables constant.

a) Subtracting the four new error functions from the original,

$$E^2(\tau_1 + \Delta, \tau_2, \alpha, \beta) - E^2(\tau_1, \tau_2, \alpha, \beta) = X$$

$$E^2(\tau_1, \tau_2 + \Delta, \alpha, \beta) - E^2(\tau_1, \tau_2, \alpha, \beta) = Y$$

$$E^2(\tau_1, \tau_2, \alpha + \Delta, \beta) - E^2(\tau_1, \tau_2, \alpha, \beta) = W$$

$$E^2(\tau_1, \tau_2, \alpha, \beta + \Delta) - E^2(\tau_1, \tau_2, \alpha, \beta) = V$$

b) Finding the square root of the sum of the squares of these remainders,

$$\overline{Z} = \sqrt{X^2 + Y^2 + W^2 + V^2}$$

c) Find the ratios

$$\frac{X}{\overline{Z}}, \quad \frac{Y}{\overline{Z}}, \quad \frac{W}{\overline{Z}}, \quad \frac{V}{\overline{Z}}$$

an increment of change H is chosen $\gg \Delta$

d) Multiply this incremental change (H) by $\frac{X}{Z}$ and change τ_1 by this amount. Similarly multiply $\frac{Y}{Z}$ times the increment $\frac{W}{Z}$ times the increment and $\frac{V}{Z}$ times the increment and add these values algebraically to the original estimates.

e) With these new values τ'_1, τ'_2, α' and β' recompute the error function and call it

f) Compute $E^2 - {}'E^2$ and proceed to form ${}''E^2$ in a similar manner from the values of ${}'E^2$, τ'_1, τ'_2, α', β' and cycle the process until ${}^{N}E^2 - {}^{N+1}E^2$ is within tolerances. The values of τ_1^{N+1}, τ_2^{N+1}, α^{N+1}, β^{N+1} are then the estimates of T_1, T_2, a, and b respectively. The value of ${}^{N}E^2 - {}^{N+1}E^2$ at which the iterative method is stopped would be determined previously.

Conditions which may be enforced in order to get a closer fit

If we no longer relax the assumption that any event occurs in general at non-integral values of spacing onthe trace and furthermore falls on a curve rather than a straight line we may come closer to the exact values of τ_1, τ_2, α, β. To utilize this information all data must be readjusted. We assumed that there is no curvature across our record and that there was no change in shape or amplitude of a wavelet from area A to area B. It is seen that these assumptions may be dropped with an increase of course in computational labor. It is felt however that the method proposed above will yield values of τ_1, τ_2, α, β which are as reliable as our seismic records permit for small angles of α and β and for non-shallow reflections.

CONCLUSIONS AND SUGGESTIONS FOR FUTURE STUDY

From the experiments concerning the inverse we may conclude that this approach will be of most use in separating two events when the onset and shape of the first are known and where the difference in onset times from that of the first wavelet to that of the second waveform does not exceed the length of the time interval during which the terms of the inverse of the first wavelet are not greatly divergent. We must further specify a low noise level. There may also be specific instances in which a form of an inverse may be used as an operator over an interval longer than itself with good results but this would depend on the occurrence of fairly singular wavelet shapes.

From the experiments concerning the use of a symmetric operator, formed from the cosine transform of the reciprocal of the amplitude spectrum of a wavelet, our conclusions are not quite as definite. The possibilities for applications of this approach, however, appear to be more numerous and more promising. With the limited experimental background we can only say that if enough data is available we can visually correlate the events spiked by the symmetric operator and neglect nill traces, considering them to be the result of phasing. It appears also that the phasing problem can be solved. Thus in the case where we have a section of a seismic record with low noise level and a complex of two similar wavelets we would expect that convolution with a symmetric operator determined for these wavelets should produce two spikes considerably larger in amplitude than the other out-put. Likewise for two different wavelets in a low noise case we expect that it will be possible to use two different operators and obtain the two spikes and hence relative times of arrival on successive convolutions.

It is suggested that the above experiments be continued

and that the least squares approach, developed qualitatively in this thesis, be set up for a digital computer and be evaluated in several experiments. From these results it is hoped that there will be conclusive evidence as to the areas of applicability and validity of each of these approaches.

REFERENCES

1. MIT Geophysical Analysis Group, Simpson, S. M. Jr., Director, 1955, Stability and physical realizability: MIT G.A.G. Report 9.

2. _____, 1956, Move-out averaging automation: MIT G.A.G. Report 10b, Section 4.

3. Bowman, Robert, 1954, An Interpretation of the published work of Norman Ricker: Special paper for MIT G.A.G.

4. Jeffreys, Harold, 1931, Damping in bodily seismic waves: Monthly Notices of the Royal Astronomical Society, Geophysics Supplement, p. 318-323.

5. Piety, R. G., 1955, Personal communication.

6. Ricker, Norman, 1953, The form and laws of propagation of seismic wavelets: Geophysics, 18, p. 10-40.

7. _____, 1953, Wavelet contraction, wavelet expansion, and the control of seismic resolution; Geophysics, 18, p. 769-792.

8. Robinson, Enders A., 1953, Evaluation of linear operators in seismogram analysis: Special paper for MIT G.A.G.

9. Treitel, Sven, 1956, Personal communication.

10. Van Melle, F. A., 1954, Note on "The primary seismic disturbance in shale": Bulletin of the Seismological Society of America, 44, p. 123-125.